Université de Montréal

Lactide Polymerization with Iron Alkoxide Complexes

par

Arek Keuchguerian

Département de chimie

Faculté des arts et des sciences

Mémoire présenté à la Faculté des études supérieures et postdoctorales

en vue de l'obtention du grade de maître des sciences (M.Sc.) en chimie

Décembre 2014

Résumé

Les essais préliminaires pour préparer des alcoolates de fer à partir du bichlorure ou bibromure de fer (II), en les combinant avec des ligands de type diimino pyridine, ont engendré la formation de complexes homoleptiques et hétéroleptiques, dépendant des substituants sur les branches imines du ligand. Ces complexes homoleptiques octaédriques et paramagnétiques ont été étudiés par rapport à leurs propriétés spectroscopiques et cristallographiques. De plus, la synthèse des complexes de fer hétéroleptique a engendré de bons précurseurs penta-coordonnés pour les réactions de substitution de ligands avec des alcoolates de métaux alcalins, de manière à produire les dialcoolates de fer (II) désirés. Des techniques d'analyse telles que la spectroscopie UV-vis, l'analyse élémentaire, la spectrométrie de masse à haute résolution et la cristallographie aux rayons X ont été utilisées pour caractériser ces complexes de fer.

L'activité catalytique de ces complexes de fer (II) a aussi été étudiée par rapport à la polymérisation du lactide; les dialcoolates convoités ont été générés *in-situ* en raison de la difficulté à produire et à isoler les dérivés alcoolates des complexes diimino pyridine de fer. Une étude approfondie a aussi été faite sur les réactions de polymérisation, surtout par rapport aux valeurs de conversion à l'échelle du temps, ainsi qu'à la tacticité des chaines de polymères obtenues. Ces analyses ont été effectuées par l'entremise de la spectroscopie de résonance magnétique nucléaire, de la chromatographie d'exclusion stérique, et de la spectrométrie de masse MALDI (désorption-ionisation laser assistée par matrice).

Mots-clés: catalyseur de fer, polymérisation de lactide, ligands diiminopyridine, polymères biodégradables, chimie verte.

Abstract

Initial attempts to prepare iron alkoxide complexes, from iron (II) dichloride or dibromide, in combination with various bis(imino) pyridine ligands, led to the formation of homoleptic and heteroleptic complexes depending on the *N*-substituents on the imino moieties. A study was made of the resulting paramagnetic octahedral homoleptic complexes, with respect to their spectroscopic properties, as well as their crystallographic parameters. Alternatively, the synthesis of penta-coordinate heteroleptic iron (II) complexes provided good precursors for the ligand substitution reactions with alkaline alkoxides, to produce the desired iron bis(alkoxide) derivatives. Methods such as UV-vis spectroscopy, elemental analysis, high resolution mass spectrometry and X-ray crystallography were used for the characterization of these iron complexes.

The catalytic activity of these iron (II) complexes was investigated with respect to lactide polymerization; the desired bis(alkoxide) species were generated *in-situ* due to the difficulties in isolating pure alkoxide derivatives of the bis(imino) pyridine iron (II) complexes. An informative study was made of both time-scale conversion values, as well as tacticity properties of the resulting polylactic acid chains, through proton nuclear magnetic resonance spectroscopy, gel permeation chromatography, as well as MALDI (matrix-assisted laser desorption/ionization) mass spectrometry measurements.

Keywords: iron catalysis, lactide polymerization, diiminopyridine ligands, biodegradable polymers, green chemistry.

Table of Contents

List of Figures

List of Tables

List of Schemes

Abbreviations

Ac	acetyl
Ar	aryl
Bn	benzyl
^{t}Bu	*tert*-butyl
CIF	crystallographic information file
d	doublet
DCM	dichloromethane
ESI	electrospray ionization
Et	ethyl
GPC	gel permeation chromatography
HRMS	high resolution mass spectrometry
L	ligand
L_{NNN}	bis(imino) pyridine ligand
m	multiplet
MALDI	matrix-assisted laser desorption ionization
Me	methyl

M_n	number-average molar mass
MS	mass spectrometry
M_w	weight-average molar mass
NMR	nuclear magnetic resonance
PDI	polydispersity
Ph	phenyl
PLA	polylactic acid
P_r	probability of obtaining racemic diads
^{i}Pr	*iso*-propyl
Py	pyridine
R	alkyl group
rac	racemic
s	singlet
t	triplet
td	triplet of doublet
THF	tetrahydrofuran
UV-vis	ultraviolet-visible

I dedicate this manuscript to my late and beloved grandmother, Linda.

Acknowledgments

I wish to express my sincere appreciation and gratitude to both my supervisors, Prof. Frank Schaper and Prof. Davit Zargarian, for the opportunity they gave me to become a member in their research groups, for the patience they showed, and for the guidance they provided over the years for the completion of this project.

I also wish to convey my heartfelt recognition and thanks to all the group members, past and present, who helped me with my work over the years, in counsel, teaching, or support. A special thanks to Berline Mougang-Soumé, who performed the crystallographic analysis and determined the X-ray structures of my compounds. I would also like to mention a special note of recognition to Pargol and Todd, for the time and energy they spent on attempting to get crystallographic data on some of my products. I would also like to express a special note of appreciation to the various research laboratories and analytical services of Université de Montréal for the use of their analytical equipment and the various analyses that were performed within the framework of this project: Prof. Garry Hanan for the use of his UV-vis spectrometer, Francine Bélanger and Michel Simard for their help and support on the acquisition of my crystallographic data, Elena Nadezhina for the elemental analysis, Dr. Alexandra Furtos, Marie-Christine Tang and Karine Venne for the mass spectrometry and MALDI analyses, and Pierre Ménard-Tremblay and Ibrahim El-Zoghbi for their help on the GPC analysis.

Last but not least, I would like to convey my heartfelt thankfulness and appreciation to my parents, Samuel and Anais, my aunt Armine, my brother Armen, and Frédéric D'Anjou, for their support at the beginning, throughout, and at the end of my M.Sc. project. Thank you!

Chapter 1

Introduction

1.1 Bis(imino) pyridine ligands

Since their first appearance in the literature in 1974,[1] tridentate Schiff bases with a pyridine backbone have become an increasingly important class of ligands. Indeed, complexes resulting from the combination of bis(imino) pyridine ligands with a variety of metal salts have led to a multitude of applications within the fields of synthetic and physical chemistry: from biological and clinical uses[2] to electrochemical and electrocatalytic properties,[3] in addition to a whole host of catalytic uses where these molecules have been applied for various polymerization reactions. The growing popularity of bis(imino) pyridine ligands can be attributed to their "ease of synthesis, potential for steric and electronic modification, and ability to serve as an electron reservoir."[4] The following two sections will endeavor to provide an overview of the synthetic and structural components and properties of bis(imino) pyridine ligands.

1.1.1 Structure and synthesis of bis(imino) pyridine ligands

One of the most important characteristics of bis(imino) pyridine ligands is the fact that their synthesis relies on a classical condensation reaction, whereby two equivalents of primary amines or anilines react with one equivalent of 2,6-diacetylpyridine or 2,6-

pyridinedicarboxaldehyde. Such a Schiff-base condensation reaction is demonstrated in the following scheme, whereby the product is a symmetrical bis(imino) pyridine ligand.

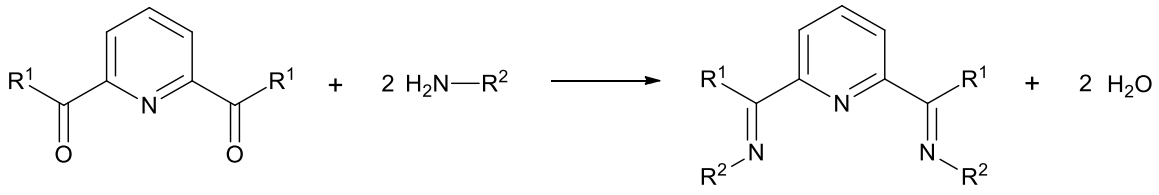

Scheme 1.1: Ligand synthesis.

Most literature sources make use of this reaction scheme by varying the R^1 substituent on the pyridine backbone between a proton, whereby making use of 2,6-pyridinedicarboxaldehyde as a starting material, or a methyl group, whereby using 2,6-diacetylpyridine; the reaction would thereby produce the desired aldimine or ketimine products, respectively. However, as it has been reported by Lappalainen *et al.*, "in the case of ketimines the reaction requires a catalytic amount of formic acid while the aldimines form without the acid. The products [precipitate] nicely from the reaction solution as yellow or white powder."[5] Also, it is worth noting that varying the R^2 substituent on the amine can allow the synthesis of a whole spectrum of bis(imino) pyridine ligands possessing varying steric properties around the imine branches of the molecule. Literature accounts of such Schiff-base condensation reactions mostly make use of anilines instead of primary amines, thereby producing 2,6-bis(arylimino) pyridine ligands with different types of substituents at the various positions around the iminophenyl rings.

Variations on the steric and electronic properties of the aniline have also been reported to affect the condensation reactions. In fact, Bryliakov and coworkers[6] clearly demonstrated this point: Schiff-base condensation of diacetylpyridine with anilines bearing electron-donating groups proceeds quite easily in solvents like ethanol or methanol, at room temperature, and with the catalytic use of carboxylic acids, whereas the same condensation reaction with anilines containing electron-withdrawing substituents requires the use of stronger acids, higher temperatures, and the careful removal of moisture from the reaction mixture.

1.1.2 Properties of bis(imino) pyridine ligands

Bis(imino) pyridine ligands have ascended in popularity and prominence not only because of their steric and synthetic adaptability, but also, as Bart *et al.* pointed out, because of their "ability to stabilize a range of transition metal and alkali metal ions."[7] In most cases, if not all, bis(imino) pyridine metal complexes are produced through simple coordination reactions, whereby the corresponding metal salts are introduced in solution with the ligand. The following scheme presents a general representation of such a coordination and complexation reaction.

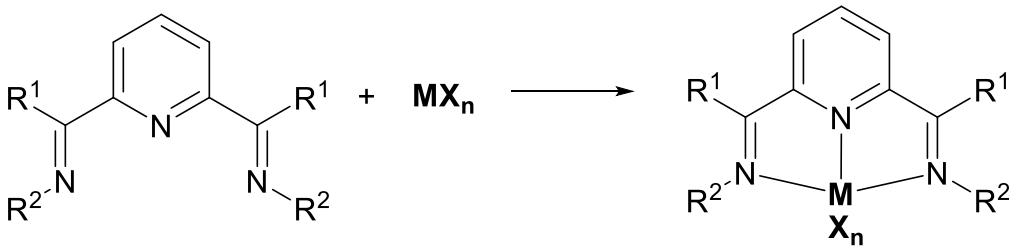

Scheme 1.2: Bis(imino) pyridine metal complex coordination.

(X = anionic ligands such as Cl^-, Br^-, etc.)

Although a number of studies have been carried out on bis(imino) pyridine metal complexes with second-row transition metals such as ruthenium,[8,9] attention has turned recently to complexes of first-row transition metals. Most notable in this domain are the works of Britovsek, Gibson and coworkers,[10] who combined bis(imino) pyridine ligands to a variety of first-row transition metals, such as titanium, vanadium, chromium, manganese, iron, cobalt and nickel. An extensive study was made of the resulting metal complexes with regards to their efficiency as ethylene polymerization catalysts. Nickel complexes with bis(imino) pyridine ligands have also been studied as catalysts for the polymerization of norbornene,[6] as well as for alkyl and aryl thiolation reactions of iodobenzene.[11] Copper and zinc complexes with bis(imino) pyridine ligands were also synthesized and their biological and antibacterial activity studied.[2]

Further attention has been devoted to the "non-innocent" electronic character of bis(imino) pyridine ligands.[9] By convention, such pincer-type molecules have usually been categorized as neutral electron-donating ligands. However, as Gallagher *et al.* pointed out, "even novice practitioners would note the possibility for substantial electron delocalization into the ligand to reduce electron density" at the coordinating metal center.[9] Others, such as Chirik and coworkers, went further, actually making use of "the ability of bis(imino) pyridines to serve as electron reservoirs," thereby "designing new catalysts or reagents for small molecule activation."[7] Prior studies had already pointed out and demonstrated how such bis(imino) pyridine ligands are not only redox active ligands that can accept up to three electrons in the anti-bonding orbitals of their conjugated π-system,[12] but also even chemically active molecules during metal-based catalytic reactions,[13] where certain alkylating agents may attack not only the imino moity of the ligand framework, but even the carbon and nitrogen atoms on the pyridine ring. Indeed, Enright *et al.* went even further in their analysis of the oxido-reductive properties of

bis(imino) pyridine ligands and explained how "the ability of the large π-system to accommodate negative charge might concurrently lead to increased Lewis acidity of the metal center, which has an obvious positive impact on catalytic performance."[12] Such properties add to the list of characteristics and attractive features that make bis(imino) pyridines an optimal ligand with respect to their use in polymerization reactions.

1.2 Iron (II) chemistry

"Iron is the second most abundant metal, after aluminum, and the fourth most abundant element in the earth's crust. The core of the earth is believed to consist mainly of iron and nickel, and the occurrence of many iron meteorites suggests that it is abundant throughout the solar system."[14] Such is the introduction given for the element of iron in Cotton and Wilkinson's *Advanced Inorganic Chemistry* reference book. It therefore comes as no surprise that iron has inspired a multitude of studies, discoveries and applications throughout the various fields of chemistry. Indeed, the potential of using iron for novel catalytic purposes has been a source of great attraction for many synthetic research groups, mainly because of its great availability, low cost and lack of toxicity.

Iron is a group 8 transition metal, with a total of eight valence shell electrons in its zero-valent state. It has been known to exist within a wide range of formsl oxidation states, from -2 to +6. However, most of the chemistry of iron involves Fe(II) or Fe(III), with only a small number of compounds that make use of Fe(IV) and Fe(VI).[15] Indeed, most of these latter compounds appear as ferrate (IV) or (VI) oxide salts, and are strong oxidizing agents. As to the configuration of iron compounds, a wide range of geometries can be observed, from trigonal planar and

tetrahedral, to octahedral and even pentagonal bipyramidal, depending on the coordination number of the metal complex itself.[14] It is worth noting, however, that most known iron (II) and iron (III) compounds are usually found with tetrahedral or octahedral geometries around the metal center.

In 1966, Ciampolini and Speroni first reported the synthesis of a five-coordinated iron (II) complex, using the bis(2-dimethylaminoethyl)methylamine tridentate ligand.[16] Indeed, "at that time, [it] was the first reported high-spin five-coordinate iron (II) complex."[17] However, it was only in 1999 that Calderazzo *et al.* actually studied and characterized the geometry of this five-coordinate iron (II) complex, which was described as severely distorted square pyramidal with one of the chlorides occupying the apical position (Fig. 1.1, left).[18] Meanwhile, van Koten[19] and Reinhoudt[20] made us of another type of tridentate ligand, 2,6-bis[(dimethylamino)methyl]pyridine, in conjunction with ruthenium and zinc complexes. It was, however, the works of Gibson and coworkers[17] that brought this ligand into prominence with regards to its complexation with iron (II) dichloride. The resulting iron (II) five-coordinate complex was thereby studied and found to also have a distorted square pyramidal geometry (Fig. 1.1, right).[17]

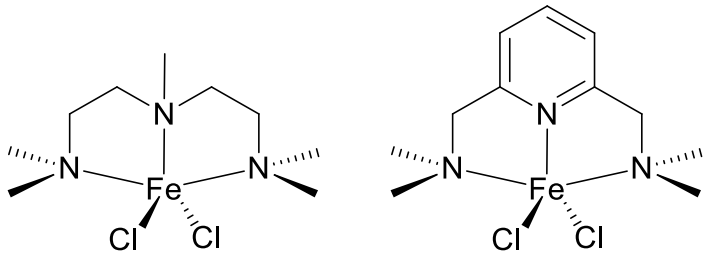

Fig. 1.1: 5-Coordinate iron (II) dichloride complexes with tridentate bis(2-dimethylaminoethyl)methylamine and 2,6-bis[(dimethylamino)methyl]pyridine ligands.

While five-coordinate iron (II) complexes were attracting increasing interest in organometallic chemistry and catalysis, bis(imino) pyridine ligands were not applied to iron chemistry until Gibson[21] and Brookhart[22] first introduced iron (II) complexes based on 2,6-bis(arylimino) pyridine ligands and reported the remarkable catalytic activities of these complexes in ethylene polymerization.

1.2.1 Bis(imino) pyridine iron (II) complexes

As mentioned above, bis(imino) pyridine iron (II) complexes were first reported in 1998 by Gibson[21] and Brookhart,[22] who independently obtained and published the crystal structure of the 2,6-diacetylpyridinebis(2,6-diisopropylanil) iron dichloride. Their reports made mention of these types of iron (II) complexes, alongside their cobalt (II) analogues, as a novel family of catalysts for the polymerization of olefins such as ethylene. Despite the lower catalytic activity of the cobalt catalysts, their study continued to grow alongside that of their analogous iron (II) complexes, which attracted increasing interest with respect to ethylene polymerization and oligomerization.

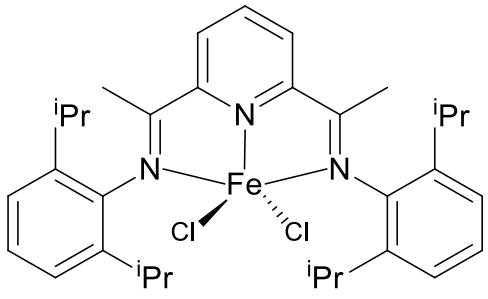

Fig. 1.2: 2,6-Diacetylpyridinebis(2,6-diisopropylanil) iron dichloride complex.

Not long after the 1998 communication, Gibson and coworkers published a full article[23] on the synthesis, structural analysis and ethylene polymerization studies of iron and cobalt catalyst systems that made use of a large variety of 2,6-bis(arylimino) pyridine ligands. Other workers, such as Abu-Surrah *et al.*, followed suit in 2002,[24] with a whole new range of bis(imino) pyridine iron (II) and cobalt (II) catalysts; new and innovative ligand structures were thereby synthesized, based on the condensation reaction of 2,6-diacetylpyridine with various types of amines, such as 1-naphtylamine, 1-aminopyrene, 2-benzylaniline, aniline and cis-myrtanylamine. Such synthetic novelties allowed the control and fine-tuning of the catalytic activity of the resulting catalyst systems. Indeed, by "varying the steric bulkiness of the aryl groups in the tridentate ligands, [a certain control was generated] of both the molecular weight and the microstructure of the resulted polyethylene."[24]

Further interesting variations were brought in with the introduction of aliphatic substituents on the imino moieties of these pincer-type ligands. Indeed, in 2005, Abu-Surrah's studies[5] brought about the synthesis of new and innovative ligand frameworks, which had been devised and synthesized through the condensation reaction of 2,6-diacetylpyridine with aliphatic amines, such as benzylamine and cyclohexanemethylamine.

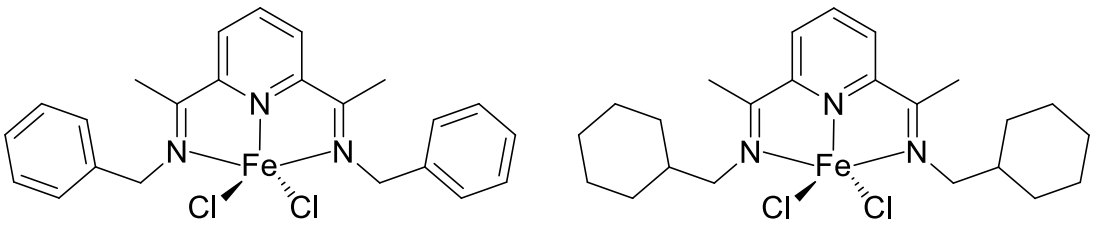

Fig. 1.3: 2,6-Bis[(benzylimino)ethyl]pyridine iron dichloride and 2,6-bis[(cyclohexanemethylimino)ethyl]pyridine iron dichloride complexes.

All these new ligands and iron (II) complexes had been properly characterized through such techniques as elemental analysis, and infra-red spectroscopy, where the vibrational stretch of the imine C=N bonds could be observed through absorption bands around 1620-1640 cm^{-1} for the ligands, and around 1530-1590 cm^{-1} for the corresponding cobalt (II) or iron (II) complexes. Crystal structures were obtained of the cobalt (II) complexes with these new ligand frameworks, where distorted trigonal bipyramidal geometries were once again observed around the metal centers. It was assumed that the corresponding iron (II) complexes would be isomorphous in terms of stereochemical structure.

In 2003, through the works of Qian and coworkers,[25,26] the first surprises were observed in the synthesis of bis(arylimino) pyridine iron (II) complexes. Indeed, until then, the synthesis of these iron (II) complexes had made use of bis(arylimino) pyridine ligands, that had been synthesized through the condensation of 2,6-diacetylpyride with various *ortho*-substituted anilines, where the *ortho*-substituents had been either a methyl or a larger group. Moreover, all crystal structures obtained for these iron (II) complexes had confirmed the 5-coordinate geometry of these complexes. However, the works of Qian made use of a fluoro-substituted 2,6-bis(arylimino) pyridine ligand.

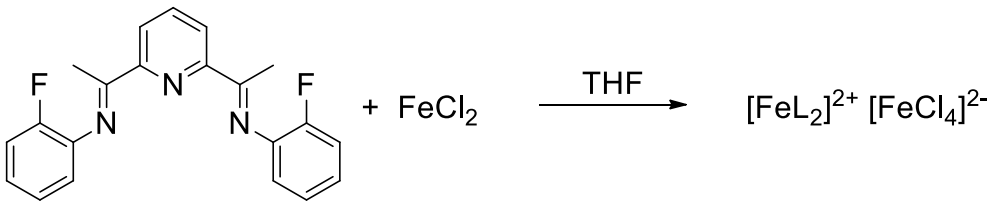

Scheme 1.3: Formation of ion-pair iron (II) complex
with 2-fluoro-substituted 2,6-bis(arylimino) pyridine ligand.

The unexpected formation of an ion-pair complex was first reported with the use of ligand systems that had been synthesized through the condensation reaction of diacetylpyridine with 2,6-difluoroaniline and 2,4-difluoroaniline[25]. Indeed, the reaction of these ligands with iron (II) dichloride had provided structures where two ligands were coordinated to a single iron atom, thereby producing a homoleptic dicationic species, with an iron tetrachloride counter-dianion. These results were validated through X-ray diffraction analysis; indeed, the crystal structure of this complex confirmed that "in the cation, the iron atom is coordinated by six nitrogen atoms from two ligands, and its coordination geometry at the iron center can be described as distorted octahedron, [whereas] the geometry at the iron center of $[FeCl_4]^{2-}$ can be described as a distorted tetrahedron."[26] No explanation was given within the works of Qian and coworkers as to the reasons behind the formation of an ion-pair complex instead of the usual 5-coordinate neutral iron (II) dichloride species.

Similar results were later observed by Ionkin *et al.* in 2006,[27,28] when the unexpected crystal structures of ion-pair iron (II) complexes were obtained through the complexation of iron dichloride with various bis(arylimino) pyridine ligands. Preliminary observations suggested that these ion-pair complexes were formed because "bis(imino)pyridine ligands with strong electron-withdrawing groups [such as nitro groups] have a tendency to bind strongly to the iron center, perhaps because of enhanced pπ-dπ back bonding interactions."[27]

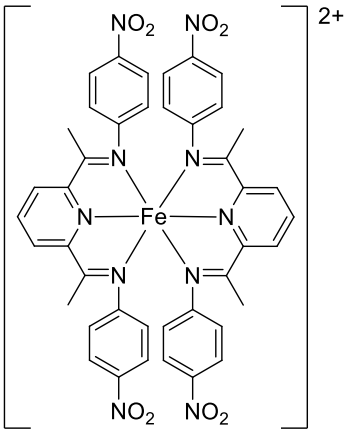

Fig. 1.4: Cationic species of ion-pair complex with nitro groups on arylimino moiety.

However, further studies of these molecules allowed Ionkin *et al.* to conclude that the lack of *ortho*-substituents on the imino aryl groups of the ligand were the reason behind the formation of ion-pair iron (II) complexes. In fact, "the presence of even one methyl group in the ortho position of the imino aryl groups in bis(imino)pyridine ligands can stabilize the formation of 1:1 complexes with distorted bipyramidal geometry."[28]

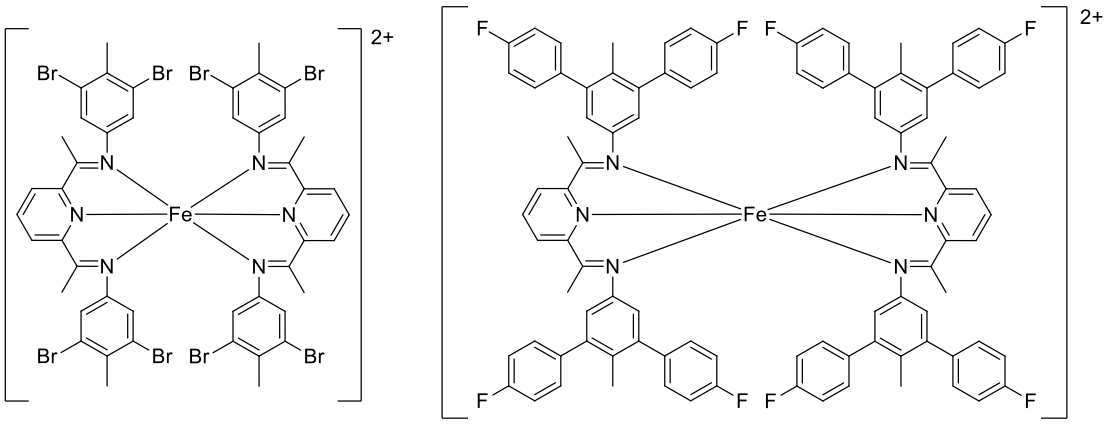

Fig. 1.5: Cationic species of ion-pair complexes $[L_2Fe]^{2+}$ $[FeCl_4]^{2-}$ as reported by Ionkin *et al.*[28]

An efficient synopsis was finally presented on the synthetic and catalytic properties of bis(imino) pyridine iron complexes by Gorl *et al.*, in 2011,[29] where iron (III) complexes were finally considered for the purpose of ethylene polymerization and oligomerization, and where a brief review was made on known iron (II) complexes. Indeed, the formation of homoleptic ion-pair iron (II) complexes was discussed, and thereby compared with the stable forms of the heteroleptic five-coordinate bis(imino) pyridine iron (II) complexes, which had previously been known and reported throughout the literature. It was finally concluded that "one of the characteristics of 2,6-bis(arylimino)pyridine iron (II) complexes is the fact that the iminophenyl rings of the ligand frameworks must contain at least one substituent at the *ortho*-position to the iminophenyl nitrogen atoms to be stable against ligand transfer reactions."[29] Interestingly enough, no mention was made of the bis(imino) pyridine iron (II) complexes with aliphatic substituents on the imino moieties, which had previously been reported by Abu-Surrah *et al.*[5] in 2005.

1.3 Lactide Polymerization

Within the context of research on biodegradable polymers, polylactide has obtained an increasing amount of importance with regards to its synthesis and properties. Indeed, plastics such as polylactic acid (PLA) are of increasing importance, not only because of their biodegradable properties, but also because of the renewable nature of its monomer source, namely lactide, which can be obtained through the fermentation of glucose, which, in turn, can be derived from corn.[30] What's more, PLA has shown great promise in a wide range of applications and commodities, from thermoplastics to films and fibers. Indeed, "the

biorenewability, biodegradability, and biocompatibility of PLA have contributed to its increasing number of applications, many of which are in the medical field."[31]

1.3.1 Polymerization and Catalysis

Given the above-stated attractive features of polylactide and its potential applications, it is no wonder that catalyst systems for the polymerization of such biocompatible polyesters have attracted much interest within the fields of catalytic green chemistry, as well as organometallic and inorganic chemistry. Such endeavors have led to increased research development and results within the design and synthesis of these biodegradable plastics, through the ring-opening polymerization mechanism of cyclic esters, namely lactide.

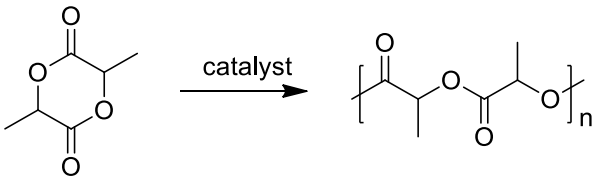

Scheme 1.4: Ring-opening polymerization of lactide.

Such a polymerization reaction is usually initiated by a metal alkoxide catalyst, and follows a coordination insertion mechanism, whereby the carbonyl oxygen undergoes coordination to the catalyst metal center. Polymerization then proceeds by the nucleophilic attack of the alkoxide at the carbonyl carbon of the lactide monomer.[32] The following scheme presents

a schematic representation of such a ring-opening polymerization mechanism that is initiated by a metal alkoxide (M-OR) catalyst complex, bearing a spectator ligand framework (Ln).

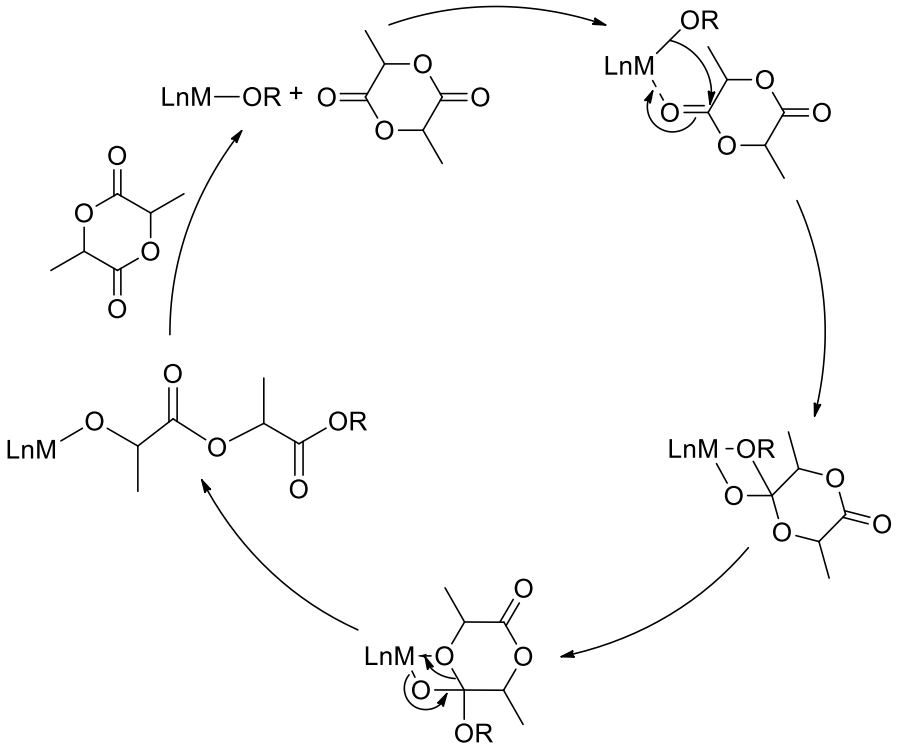

Scheme 1.5: Ring-opening polymerization of lactide initiated by a metal alkoxide.

A wide variety of metals has been studied as potential catalyst systems for the ring-opening polymerization of lactide. Some of the earlier studies have considered aluminum alkoxide complexes as suitable initiators for lactide polymerization.[33] Zinc[34] and magnesium[35] alkoxide complexes later appeared as efficient catalysts, with a wide variety of ligand frameworks around the metal center. An important factor in the design of efficient catalyst

systems appeared to be the coordinative unsaturation around the metal center, in order to allow initiation of the polymerization through the coordination of lactide to the metal center.

Studies on zinc and magnesium complexes as single-site catalysts for the ring-opening polymerization of lactide also demonstrated the efficient use of diketiminate ligands around the metal centers.[36,37] Such a ligand framework was also used by Gibson and coworkers in the synthesis of an active tin (II) metal complex catalyst system.[38] Using *N*-alkyl diketiminate ligands, Schaper and coworkers obtained exceptionally active catalyst systems with zirconium[40] and copper[41] as metal centers, bearing novel diketiminate ligand frameworks. Such studies clearly fall into the pattern and general scheme of using metals with low cytotoxicity levels for the manufacture of new and active catalyst systems for the ring-opening polymerization of lactide. Within such a framework of environmental considerations, attention was also given to iron, for the design of new metal alkoxide complexes for the polymerization of lactide.

1.3.2 Iron in lactide polymerization

The design of new catalyst systems for the polymerization of lactide based on iron as an active metal center have recently attracted a great deal of interest. This is mainly due to the non-toxic and biocompatible nature of iron. Indeed, Gibson and coworkers made a very important point with regards to this issue, by providing the following explanation in their 2003 publication.

> "Depending on the method of production, it is not always possible to ensure complete removal of metal-catalyst residues from the resultant polymer. Clearly, when the polylactide material is intended for biomedical or food-packaging applications, the use of initiators based on toxic metals is undesirable, and there is

consequently considerable interest in designing initiators based on low-toxicity metals for the controlled polymerization of cyclic esters."[32]

Within the framework of research in this direction, the use of iron (II) complexes has triggered surprisingly little interest. Some of the first examples of iron (II) catalyst systems for lactide polymerization involved iron porphyrin[42] and iron acetate[43] complexes. However, these iron (II) compounds did not demonstrate great activity or efficiency in terms of polymerization catalysis. Attention was later turned to iron (III) alkoxides, with the works of O'Keefe *et al.*, [44] who first reported the synthesis and catalytic study of homoleptic dinuclear ferric alkoxide complexes (Fig. 1.6). Such compounds exhibited moderately high catalytic activity with regards to cyclic ester polymerization, but also showed mechanistic and kinetic complications due to the multiple-site catalyst nature of the compounds.

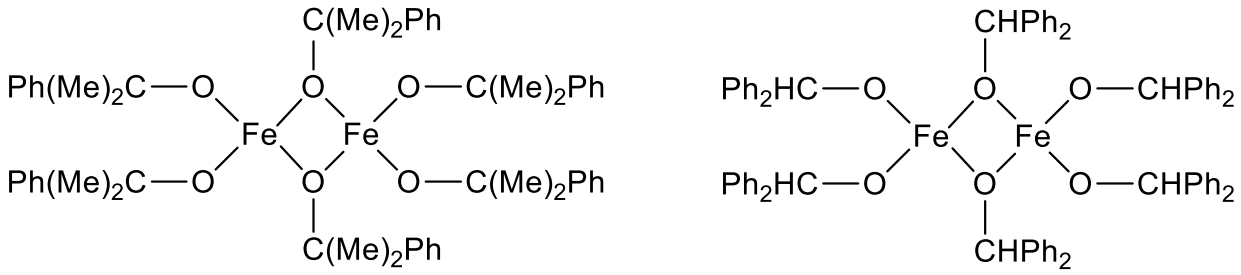

Fig. 1.6: Homoleptic dinuclear iron (III) alkoxide complexes as reported by O'Keefe *et al.*[44, 30]

Later studies by O'Keefe *et al.*[30] revealed the synthesis of new mononuclear heteroleptic iron (III) alkoxide complexes, and compared such single-site catalysts to the earlier homoleptic

dinuclear compounds. Despite their simple first-order kinetic behavior, these new mononuclear single-site catalysts showed poor polymerization activity.

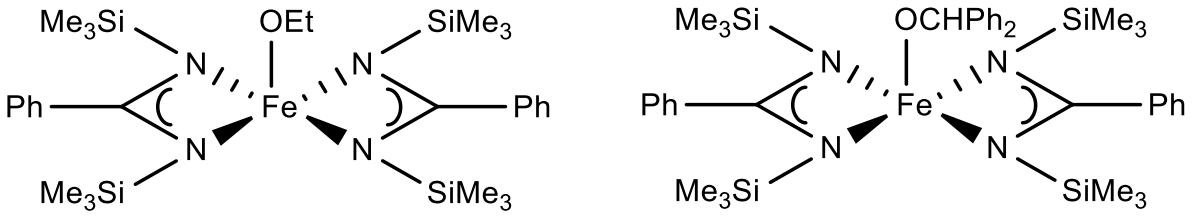

Fig. 1.7: Heteroleptic mononuclear iron (III) alkoxide complexes as reported by O'Keefe *et al.*[30]

Further studies on iron (II) alkoxide initiators, for the controlled polymerization of lactide, brought about the synthesis and catalytic study of a novel tridentate iron (II) complex by Gibson *et al.*,[45] using a diketiminate ligand framework around the metal center.

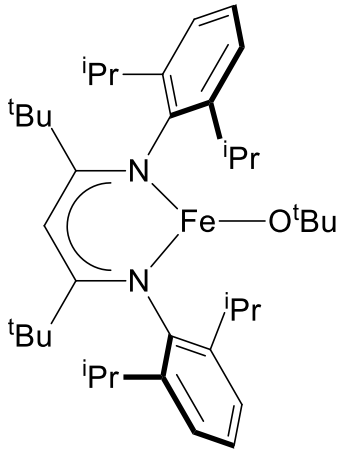

Fig. 1.8: Iron (II) diketiminate alkoxide complex as reported by Gibson *et al.*[45]

Such a system was thereby easily compared to previous catalyst systems, which also made use of such ligand frameworks, with others metals, such as zinc, magnesium and tin. Preliminary conclusions reported that "the activity of this iron (II) system for lactide polymerization is comparable to its zinc (II) relative, and occupies a position amongst the most active systems for controlled lactide polymerization."[45] As such, later studies by Gibson and coworkers expanded over other types of ferrous alkoxide compounds, such as anionic iron (II) alkoxide heterometallic complexes.[32]

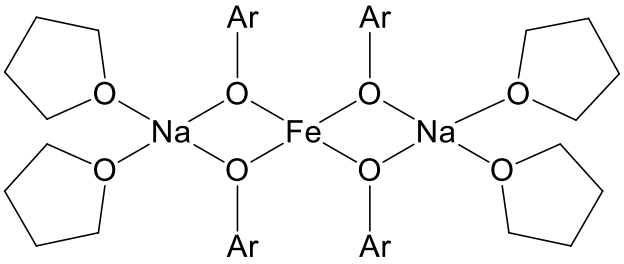

Fig. 1.9: Iron (II) heterometallic alkoxide complex as reported by Gibson and coworkers.[32]

Studies around such iron (II) alkoxide systems clearly established these compounds as effective initiators for the ring-opening polymerization of lactide. However, despite such promising preliminary results, many questions were left unanswered with respect to the mechanistic and kinetic study and control of lactide polymerization reactions using iron (II) alkoxide catalyst systems. Moreover, a definite lack of information could be observed with

regards to the role of the ligand framework within the catalytic process, in terms of both the steric control over the geometry of the iron compound, as well as any catalytic-site control.

1.3.3 Bis(imino) pyridine iron complexes in lactide polymerization

Soon after the experimental work on the project presented in this manuscript was completed, Byers and coworkers reported the use of five-coordinate iron (II) alkoxides, for the catalysis of lactide polymerization.[46] Their initial synthetic endeavors demonstrated the problematic and challenging nature of the synthesis of such iron (II) complexes. Indeed, their original scheme proposed making the desired complexes through the salt metathesis reaction between a bis(imino) pyridine iron dichloride complex and sodium alkoxides. However, such a scheme usually resulted in a decomposition of the reagents, and an impossibility to isolate and characterize any desirable product whatsoever.

The desired five-coordinate iron (II) alkoxide species were finally obtained through protonolysis reactions of the corresponding dialkyl complexes with various aromatic and aliphatic alcohols. These bis(imino) pyridine bis(alkoxide) iron complexes were reportedly obtained in high yields, and, although no elemental analysis and crystallographic data could be obtained for these products, the process of protonation could be neatly followed via proton NMR spectroscopy. Further characterization was done through the crystallographic data of a cationic iron (III) derivative of one of the iron (II) bis(alkoxide) complexes, which was obtained through the oxidation of the iron (II) alkoxide with ferrocenium hexafluorophosphate. The trigonal bipyramidal geometry of the resulting iron (III) five-coordinate complex was thus confirmed.

The catalytic activity of these iron (II) alkoxide complexes, toward the polymerization of lactide at room temperature was also investigated by Byers and coworkers. Polymerization conversions of up to 93% were obtained after 3 hours of reaction, with monomer to catalyst ratios of 50:1. In addition to the various molecular weight and polydispersity measurements, the authors also performed a number of *in-situ* experiments, where the active alkoxide species were formed prior to the polymerization reactions by treating the iron (II) dialkyl precursor complex with an alcohol. It goes without saying, of course, that the authors investigated a number of different alcohols as initiators for the catalytic polymerization of lactide, ranging from various phenols to benzyl alcohols and neopentyl alcohol, which "was found to be the most efficient initiator of all that were studied […], although this initiator resulted in significantly lower molecular weight polymer."[46]

All in all, the article by Byers and coworkers produced a new stepping stone for the synthesis and development of iron (II) catalyst systems for the efficient polymerization of lactide. Iron (II) complexes bearing bis(imino) pyridine ligand frameworks were used and featured for the first time within the context of lactide polymerization. Moreover, their results showed promising new avenues for the development and study of newer and even more efficient catalyst systems, based on iron (II) complexes bearing the same framework.

Despite all the above-noted promising new reports and reviews, the study of iron (II) complexes for lactide polymerization still remains underdeveloped, in comparison to some of the older and more prominent catalytic systems that are based on other metals, such as zinc, magnesium and tin, and which have been studied with far more depth and experience.

1.4 Aim of the project

The main objective of this project is to investigate the synthesis and development of new pincer-like five-coordinate iron-based catalysts for the polymerization of lactide. Within such a context, we are interested in the conception and synthesis of precursor iron (II) complexes that are based on tridentate bis(imino) pyridine ligands. The desired bis(alkoxide) iron catalysts could then be prepared through the salt metathesis reaction between these precursor iron (II) complexes and alkaline metal alkoxides.

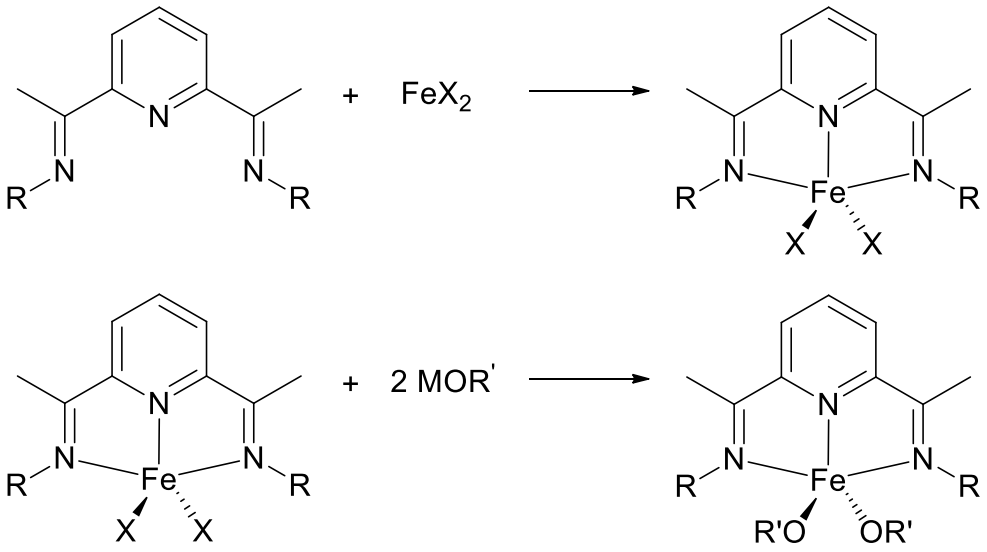

Scheme 1.6: Targeted iron (II) catalyst system.

As mentioned above, one of the most important factors in the design of new and efficient catalyst systems for lactide polymerization is the coordinative unsaturation around the metal center. As such, five-coordinate iron complexes clearly fall within the framework of such a

scheme, since they would presumably allow easy monomer coordination to the metal center, to possibly form intermediate six-coordinate complexes. Moreover, the great availability, low cost and lack of toxicity of iron itself makes it into a more than adequate candidate for the catalytic polymerization of lactide.

Bis(imino) pyridine ligands are particularly attractive, in view of the numerous literature accounts that make use of such ligand frameworks within catalytic polymerizations.[21-24] The synthesis itself of these ligands offers the advantageous possibility of varying the steric properties around the imine branches of the molecule simply by using different amine reagents. As such, we intend to investigate flexible ligand frameworks using *N*-alkyl substituents, as well as their more rigid *N*-aryl analogues.

1.5 References

(1) Alyea, E. C.; Merrell, P. H. *Synthesis and Reactivity in Inorganic and Metal-Organic Chemistry*, **1974**, 4, 535.

(2) Gehad, G. M. *Spectrochim. Acta*, **2006**, 64, 188-195.

(3) Chiericato, G. Jr.; Arana, C. R.; Casado, C.; Cuadrado, I.; Abruna, H. D. *Inorg. Chim. Acta*, **2000**, 300-302, 32-42.

(4) Thammavongsy, Z.; Seda, T.; Zakharov, L. N.; Kaminsky, W.; Gilberston, J. D. *Inorg. Chem.*, **2012**, 51, 9168-9170.

(5) Lappalainen, K.; Yliheikkila, K.; Abu-Surrah, A. S.; Polamo, M.; Leskela, M.; Repo, T. *Z. Anorg. Allg. Chem.*, **2005**, 631, 763-768.

(6) Antonov, A. A.; Semikolenova, N. V.; Zakharov, V. A.; Zhang, W.; Wang, Y.; Sun, W.-H.; Talsi, E. P.; Bryliakov, K. P.; *Organometallics*, **2012**, 31, 1143-1149.

(7) Bart, S. C.; Chlopek, K.; Bill, E.; Bouwkamp, M. W.; Lobkovsky, E.; Neese, F.; Wieghardt, K.; Chirik, P.J. *J. Am. Chem. Soc.*, **2006**, 128, 13901-13912.

(8) Cetinkaya, B.; Cetinkaya, E.; Brookhart, M.; White, P. S. *J. Mol. Catal. A: Chem.*, **1999**, 142, 101-112.

(9) Gallagher, M.; Wieder, N. L.; Dioumaev, V. K.; Carroll, P. J.; Berry, D. H. *Organometallics*, **2010**, 29, 591-603.

(10) Smit, T. M.; Tomov, A. K.; Britovsek, G. J. P.; Gibson, V. C.; White, A. J. P.; Williams, D. J. *Catal. Sci. Technol.*, **2012**, 2, 643-655.

(11) Baldovino-Pantaleon, O.; Hernandez-Ortega, S.; Morales-Morales, D. *Inorg. Chem. Commun.*, **2005**, 8, 955-959.

(12) Enright D.; Gambarotta, S.; Yap, G. P. A.; Budzelaar, P. H. M. *Angew. Chem., Int. Ed.*, **2002**, 41, 3873-3876.

(13) Bruce, M.; Gibson, V. C.; Redshaw, C.; Solan, G. A.; White, A. J. P.; Williams, D. J. *Chem. Commun.*, **1998**, 2523-2524.

(14) Cotton, F. A.; Wilkinson, G., *Advanced Inorganic Chemistry: A Comprehensive Text*, 2nd ed.; John Wiley & Sons, Inc., **1966**, 849.

(15) Housecroft, C. E.; Sharpe, A. G., *Inorganic Chemistry*, 3rd ed.; Pearson Education Ltd., **2008**, 714.

(16) Ciampolini, M.; Speroni, G. P. *Inorganic Chemistry*, **1966**, 5, 45-49.

(17) O'Reilly, R. K.; Gibson, V. C.; White, A. J. P.; Williams, D. J. *Polyhedron*, **2004**, 23, 2921-2928.

(18) Calderazzo, F.; Englert, U.; Pampaloni, G.; Vanni, E. *C. R. Acad. Sci. Paris*, **1999**, 311.

(19) Del Rio, I.; Gossage, R. A.; Hannu, M. S.; Lutz, M.; Spek, A. L.; van Koten, G. *Organometallics*, **1999**, 18, 1097-1105.

(20) Molenveld, P.; Stikvoort, W. M. G.; Koojiman, H.; Spek, A. L.; Engbersen, J. F. J.; Reinhoudt, D. N. *J. Org. Chem.*, **1999**, 64, 3896-3906.

(21) Britovsek, G. J. P.; Gibson, V. C.; Kimberley, B. S.; Maddox, P. J.; McTavish, S. J.; Solan, G. A.; White, A. J. P.; Williams, D. J. *Chem. Commun.*, **1998**, 849.

(22) Small, B. L.; Brookhart, M.; Bennett, A. M. A. *J. Am. Chem. Soc.* **1998**, 120, 4049-4050.

(23) Britovsek, G. J. P.; Bruce, M.; Gibson, V. C.; Kimberley, B. S.; Maddox, P. J.; Mastroianni, S.; McTavish, S. J.; Redshaw, C.; Solan, G. A.; Stromberg, S.; White, A. J. P.; Williams, D. J. *J. Am. Chem. Soc.*, **1999**, 121, 8728-8740.

(24) Abu-Surrah, A. S.; Lappalainen, K.; Piironen, U.; Lehmus, P.; Repo, T.; Leskela, M. *J. Org. Chem.*, **2002**, 648, 55-61.

(25) Chen, Y.; Qian, C.; Sun, J. *Organometallics*, **2003**, 22, 1231-1236.

(26) Chen, Y.; Chen, R.; Qian, C.; Dong, X.; Sun, J. *Organometallics*, **2003**, 22, 4312-4321.

(27) Ionkin, A. S.; Marshall, W. J.; Adelman, D. J.; Shoe, A. L.; Spence, R. E.; Xie, T. *J. Polym. Sci., Part A: Polym. Chem.*, **2006**, 44, 2615-2635.

(28) Ionkin, A. S.; Marshall, W. J.; Adleman, D. J.; Fones, B. B.; Fish, B. M.; Schiffhauer, M. F. *Organometallics*, **2006**, 25, - 2978-2992.

(29) Gorl, C.; Englmann, T.; Alt, H. G. *Appl. Catal. A: Gen.*, **2011**, 403, 25-35.

(30) O'Keefe, B. J.; Breyfogle, L. E.; Hillmyer, M. A.; Tolman, W. B. *J. Am. Chem. Soc.*, **2002**, 124, 4384-4393.

(31) Chen, H.-Y.; Mialon, L.; Abboud, K. A.; Miller, S. A. *Organometallics*, **2012**, 31, 5252-5261.

(32) McGuinness, D. S.; Edward, L. M.; Gibson, V. C.; Steed, J. W. *J. Polym. Sci., Part A: Polym. Chem.*, **2003**, 41, 3798-3803.

(33) Kowalski, A.; Duda, A.; Penczek, S. *Macromolecules*, **1998**, 31, 2114-2122.

(34) Cheng, M.; Attygalle, A. B.; Lobkovsky, E. B.; Coates, G. W. *J. Am. Chem. Soc.*, **1999**, 121, 11583-11584.

(35) Chisholm, M. H.; Eilerts, N. W.; Huffman, J. C.; Iyer, S. S.; Pacold, M.; Phomphrai, K. *J. Am. Chem. Soc.*, **2000**, 122, 11845-11854.

(36) Chamberlain, B. M.; Cheng, M.; Moore, D. R.; Ovitt, T. M.; Lobkovsky, E. B.; Coates, G. W. *J. Am. Chem. Soc.*, **2001**, 123, 3229-3238.

(37) Chrisholm, M H.; Huffman, J. C.; Phomphrai, K. *J. Chem. Soc., Dalton Trans.*, **2001**, 222-224.

(38) Dove, A. P.; Gibson, V. C.; Marshall, E. L.; White, A. J. P.; Williams, D. J. *Chem. Commun.*, **2001**, 283-284.

(39) Drouin, F.; Oguadinma, P. O.; Whitehorne, T. J. J.; Prud'homme, R. E.; Schaper, F. *Organometallics*, **2010**, 29, 2139-2147.

(40) El-Zoghbi, I.; Whitehorne, T. J. J.; Schaper, F. *Dalton Trans.*, **2013**, 42, 9376-9387.

(41) Whitehorne, T. J. J.; Schaper, F. *Inorg. Chem.*, **2013**, 52, 13612-13622.

(42) Kricheldorf, H. R.; Beottcher, C. *Makromol. Chem.*, **1993**, 194, 463-473.

(43) Stolt, M.; Sodergard, A. *Macromolecules*, **1999**, 32, 6412-6417.

(44) O'Keefe, B. J.; Monnier, S. M.; Hillmyer, M. A.; Tolman, W. B. *J. Am. Chem. Soc.*, **2001**, 123, 339-340.

(45) Gibson, V. C.; Marshall, E. L.; Navarro-Llobet, D.; White, A. J. P.; Williams, D. J. *J. Chem. Soc., Dalton Trans.*, **2002**, 4321-4322.

(46) Biernesser, A. B.; Li, B.; Byers, J. A. *J. Am. Chem. Soc.*, **2013**, 135, 16553-16560.

Chapter 2

Lactide Polymerization with Iron Alkoxide Complexes

Arek Keuchguerian, Berline Mougang-Soume, Frank Schaper[1] and Davit Zargarian*[2]*

Centre in Green Chemistry and Catalysis,

Département de chimie, Université de Montréal

Keywords : iron catalysis, lactide polymerization, diiminopyridine ligands, biodegradable polymers, green chemistry

2.1 Abstract

This report presents the results of a study on the preparation of iron alkoxide complexes chelated by diiminopyridine ligands and their role in the room temperature polymerization of *rac*-lactide. Reaction of *N*,*N*'-(*p*-R-$C_6H_4CH_2$)$_2$-diiminopyridines (R = H (**1**), F (**2**)) with FeX_2 (X = Cl, Br) yielded the homoleptic complexes [(**1**)$_2$Fe][FeX_4] or [(**2**)$_2$Fe][FeX_4], respectively. Treating the latter with Na[BPh_4] afforded the anion exchange product [(**2**)$_2$Fe][BPh_4]$_2$, which was characterized by ^{1}H NMR and absorption spectroscopy, combustion analysis, and single crystal X-ray diffraction. Various attempts to grow crystals of [(**1**)$_2$Fe][FeX_4] and [(**2**)$_2$Fe][FeX_4] culminated in the isolation of single crystals of [(**2**)$_2$Fe][Cl_6Fe_2O], which was characterized by X-ray diffraction. Attempted synthesis of well-defined, mononuclear alkoxide derivatives from [(**1**)$_2$Fe]$^{2+}$ or [(**2**)$_2$Fe]$^{2+}$ gave mostly intractable products, but in one case we obtained the crystallographically characterized sodium iron cluster $Na_4Fe_2(OC_6H_4F)_8(THF)_2$. An aryloxide derivative proved accessible by reaction of $NaOC_6H_4F$ with the mono-ligand precursor $LFeCl_2$ (L= *N*,*N*'-dimesityl-diiminopyridine), but characterization of $LFe(OC_6H_4F)_2$ was limited to a single crystal X-ray diffraction analysis due to unsuccessful attempts at isolating pure samples. The difficulties encountered in isolation of pure alkoxide derivatives prompted us to use in-situ generated $LFe(OEt)_2$ for studying polymerization of *rac*-lactide. This system was found to be moderately active at room temperature and with a slight preference for formation of heterotactic polymer (P_r = 0.54-0.65). Large polydispersities of 1.5-2.0 indicated the presence of transesterification side reactions, which were confirmed by the presence of peaks with $m/z = n\cdot 144 + M(\text{EtOH}) + M(Na^+)$ and $m/z = (n+0.5)\cdot 144 + M(\text{EtOH}) + M(Na^+)$ in MALDI-MS.

2.2 Introduction

Polylactide, a marketed polymer of lactic acid obtained by ring-opening polymerization of lactide,[1] has gained interest due to its potential biodegradability and availability from renewable resources.[2-4] The currently practiced industrial production of polylactide is based on polymerization of enantiopure lactide catalyzed by a non-selective tin octoate precursor,[1] but much effort has been invested recently to develop improved catalysts for the conversion of *rac*-lactide to polymers with controlled molecular weight, polydispersity and stereochemistry (tacticity). Many high-activity catalysts of this type have been reported, including systems based on alkaline, earth alkaline, rare-earth and early-transition metals.[1, 5-11] Catalysts based on group 13 elements Al, Ga, and In often display low activities, but these systems have attracted interest thanks to their often high isoselectivity.[8, 12-14]

With regard to late-transition-metal catalysts, the seminal work of Coates and coworkers[15] has led to extensive investigation of zinc complexes.[5] Recent reports from the Schaper group have also introduced several highly active catalysts based on Cu.[16-18] On the other hand, far fewer reports have appeared on development of catalytic systems based on mid-first-row transition metals.[19-21] For instance, we are aware of only a handful of reports on lactide polymerization with iron coordination complexes.[22-25] This paucity of data on the potential lactide polymerization activities of Fe(II)-based catalysts, combined with the great abundance and low toxicity of this metal, prompted us to explore the preparation of LFe(OR) complexes and their aptitude for *rac*-lactide polymerization. Herein we report our initial attempts to prepare heteroleptic iron alkoxide complexes with diiminopyridine ligands and study their reactivities in *rac*-lactide polymerization.

2.3 Results and Discussion

Complexes with *N*-benzyl substituents. The tridentate *N*-benzyl ligands **1** and **2** were obtained by condensation of bis(acetyl)pyridine with the appropriate amine (Scheme 2.1). Reaction of these ligands with FeX_2 (X = Cl or Br) led to the formation of paramagnetic compounds **3**-**6** (Scheme 1), which were characterized as follows. The elemental analyses of these compounds agreed with the general formula "(**1**)FeX_2" (**3** and **5**) or "(**2**)FeX_2" (**4** and **6**), but the ESI-MS data were not consistent with heteroleptic complexes, showing only masses belonging to homoleptic bis(ligand) species of the type $[L_2Fe]^{2+}$ (in the positive ion mode) and $[FeX_4]^{2-}$ (in the negative ion mode, see experimental part). Since it seemed unlikely that these homoleptic species $[L_2Fe][FeX_4]$ would form via a bimolecular ligand redistribution pathway under MS analysis conditions, we concluded that the complexes **3-6** were obtained as homoleptic ion pairs. Despite several attempts to grow crystals of **3-6**, X-ray suitable crystals were obtained only in one case: complex **4b**, obtained from crystallization of **4**, was found to consist of $[(\mathbf{2})_2Fe]^{2+}$ cations and $[Cl_3FeOFeCl_3]^{2-}$ anions, the latter originating from oxidation during crystallization (Table 2.1 and Supporting Information).

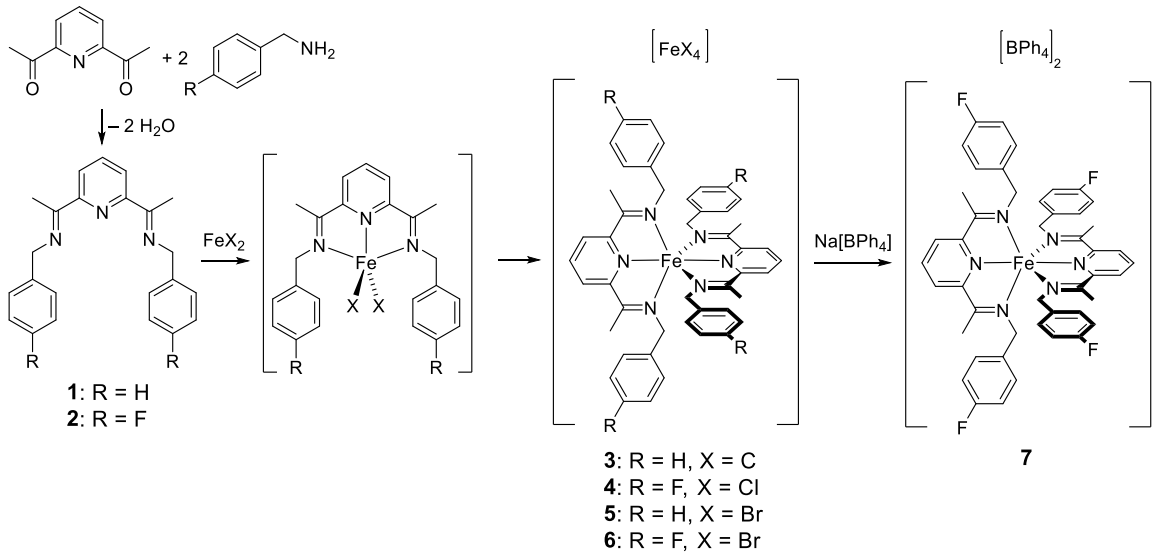

Scheme 2.1

The presence of homoleptic ion pairs in **3-6** was further supported by the preparation of diamagnetic $[(\mathbf{2})_2Fe][BPh_4]_2$, **7**, obtained in 91% yield from the reaction of $FeCl_2$ with **2**, followed by treatment with $NaBPh_4$ (Scheme 2.1). Compound **7** was convincingly characterized by combustion analysis, ^1H NMR and UV-vis spectroscopy (vide infra).

Single crystals of **7**, obtained by recrystallization from acetonitrile, allowed a definitive characterization of this compound by X-ray diffraction analysis (Fig. 2.1). Inspection of the metric parameters for **7** and **4b** (Table 2.1) reveals that the two dications share a practically identical geometry despite the different counteranions and the crystallographic C_2-symmetry in **7**. The iron center adopts a slightly distorted octahedral environment due to the decreased bite angle of the five-membered metallacycle of ≈80°. The Fe-N bond length to the central pyridine is 0.10 Å shorter than those to the two imine

nitrogen atoms; this is typically observed for diiminopyridine iron complexes (0.06 – 0.25 Å, based on 60 structures)[26] and terpyridine iron complexes (0.03 – 0.33 Å, based on 64 structures)[26] to compensate for the deviation of the bite angle from ideal octahedral geometry. Coordination geometry around the metal center is otherwise unremarkable and bond distances and angles are well in the range typically observed for octahedral diiminopyridine iron complexes (Fe-N_{Py} = 1.80 – 2.22 Å, Fe-N_{imine} = 1.90 – 2.28 Å, N_{Py}-Fe-N_{imine} = 73 – 81°).[27-36]

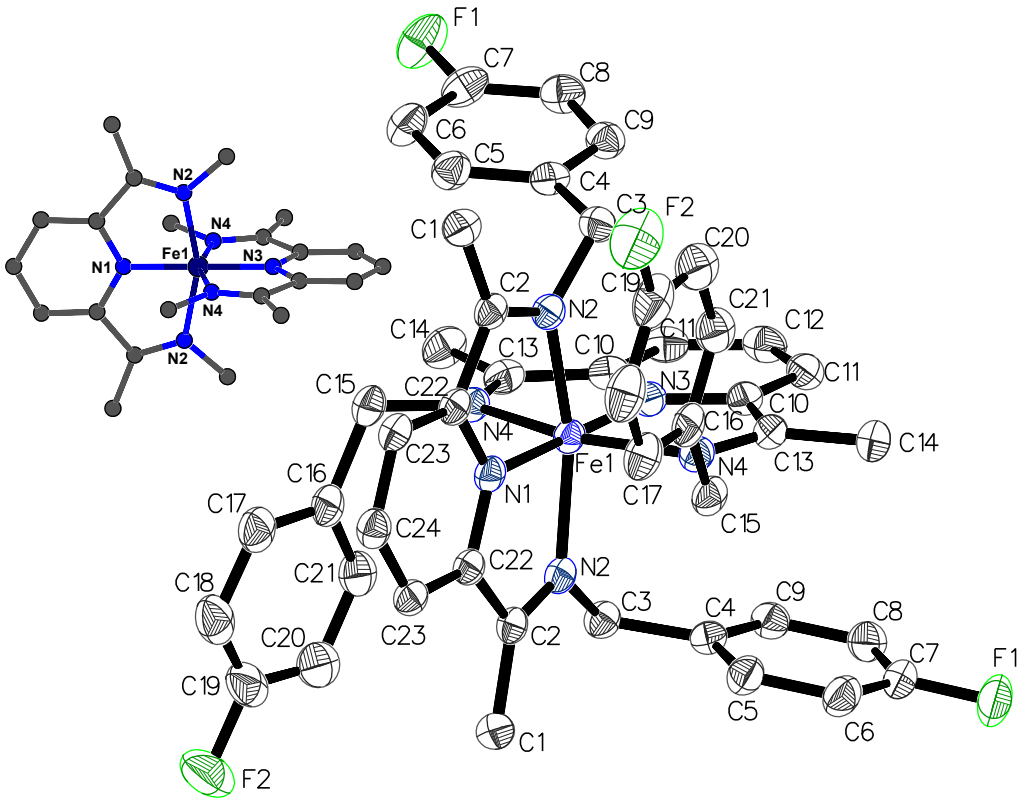

Fig. 2.1: Crystal Structure of **7**. Thermal ellipsoids are drawn at 50% probability. Hydrogen atoms, cocrystallized solvent and the $[BPh_4]^-$ anions are omitted for clarity. The inset diagram shows the molecule with the benzyl substituents omitted.

Table 2.1: Bond distances (Å) and angles (°) for [(**2**)$_2$Fe]X

	4b	**7**
Fe-N_{Py}	1.872(2), 1.872(2)	1.871(2), 1.873(2)
Fe-N_{imine}	1.973(2) – 1.990(2)	1.979(1), 1.981(1)
N_{Py}-Fe-N_{imine}	79.55(7) – 79.71(7)	79.71(4), 79.70(4)
N_{imine}-Fe-$N_{imine,\ trans}$	159.26(7), 159.41(7)	159.43(8), 159.39(8)
N_{imine}-Fe-$N_{imine,\ cis}$	91.42(7) – 92.54(7)	90.64(5), 93.02(5)
N_{Py}-Fe-N_{Py}	178.37(8)	180

Compound **7** was thus unambiguously assigned as a homoleptic cationic iron complex. Comparison of the UV-vis spectrum of this diamagnetic species (Fig. 2.2) to those of paramagnetic species **3-6** showed that the only notable differences among these complexes occurred in the high-energy transition ranges (350–450 nm), the low-energy transitions being practically identical with only minor variations (±20%) in molar absorbance. While it might be tempting at first sight to assign these additional absorptions to the presence of $[FeX_4]^{2-}$ anions, the latter do not show any notable absorption in the visible region.[37-38] Nevertheless, comparison of the obtained UV/vis spectra, in combination with mass spectrometry results has allowed us to identify **3-6** unambiguously as homoleptic ion-paired complexes of the type $[L_2Fe][FeX_4]$.

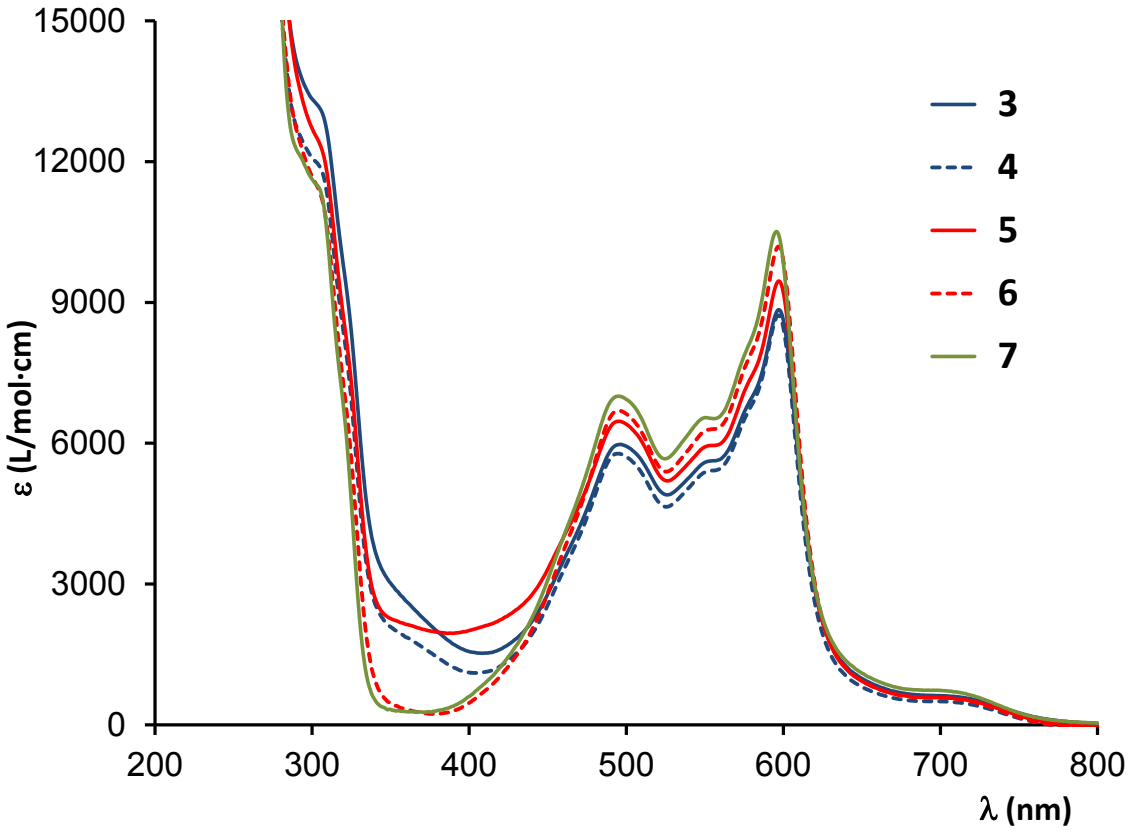

Fig. 2.2: UV/vis spectra of **3**-**7** in ethanol.

Attempts to prepare heteroleptic (L)Fe(OR)$_2$ by treating **3** or **4** with two equivalents of NaOEt or NaOC$_6$H$_4$F did not lead to any isolable products, but a single crystal was obtained from a reaction of **4** with excess NaOC$_6$H$_4$F. As shown in Figure 2.3, this product turned out to be the sodium-iron cluster Na$_4$Fe$_2$(OC$_6$H$_4$F)$_8$(THF)$_2$ formed by elimination of the tridentate ligand **2**. The cluster is defined by two symmetry equivalent iron centers coordinated by phenolate ligands in a tetrahedral environment. The net negative charge of the Fe(II)O$_4$ fragments is counter-balanced by four sodium cations that coordinate to the phenolate oxygen atoms and form two face-sharing open cubes (Fig. 2.3). The sodium atoms attain penta- and hexa-coordination environments by

coordination of THF and the *para*-fluorine substituents from neighboring clusters (Fig. 2.3, top, Supporting Information).

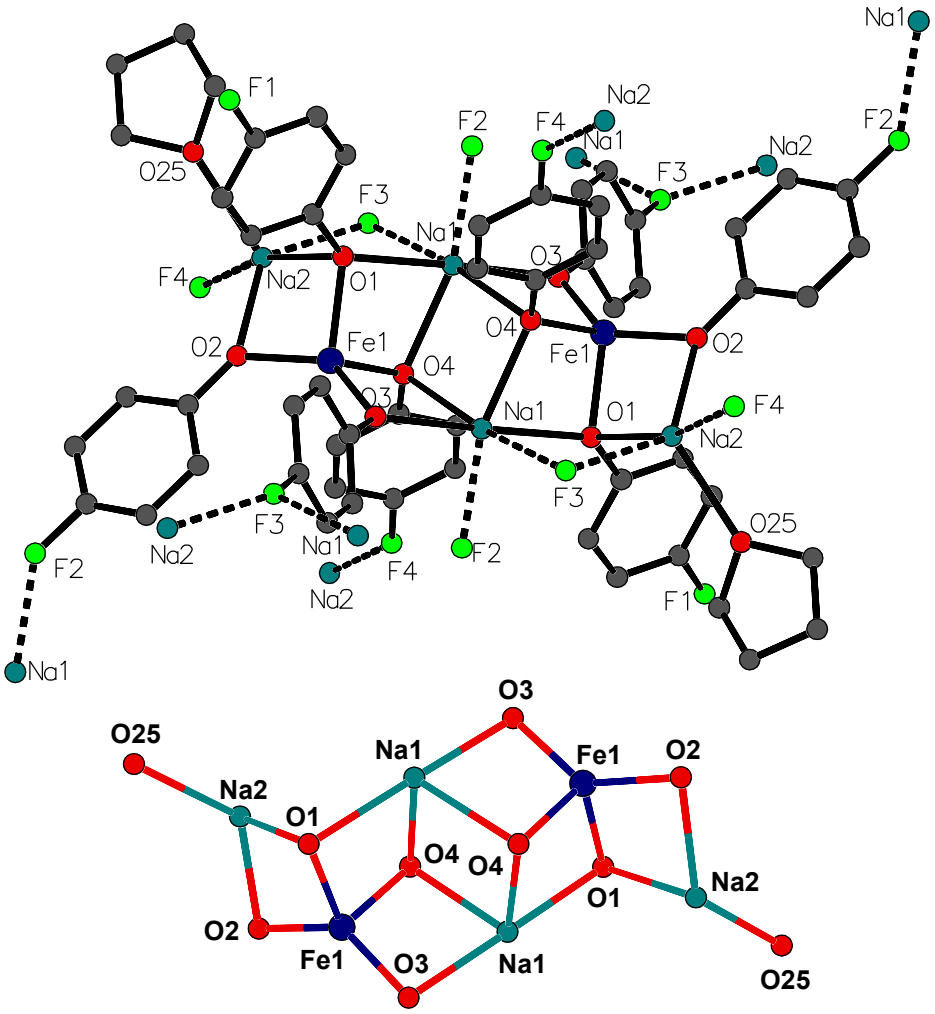

Fig 2.3: Top: Crystal structure of the $Na_4Fe_2(OC_6H_4F)_8(THF)_2$ cluster. Hydrogen atoms and the minor parts of disordered THF and phenolate ligands are omitted for clarity. Broken lines indicate intermolecular coordination to neighboring molecules. Bottom: The $Na_4Fe_2O_{10}$ core of the cluster with the two face-sharing open cubes. Selected geometrical data: Fe-O: 1.926(3) - 2.035(3) Å, Na-OC_6H_4F: 2.326(3) - 2.471(3) Å, Na-F: 2.325(3) - 2.550(3) Å, O-Fe-O: 90.3(1) – 134.9(1)°.

Given our unsuccessful attempts to prepare (L_{NNN})FeX_2 complexes (L_{NNN} = diiminopyridine), it is worth noting that the preparation of (**1**)$FeCl_2$ has been reported previously, albeit without structural characterization.[39] However, other authors have likewise noted the tendency of (L_{NNN})FeX_2 complexes to undergo ligand re-distribution reactions that culminate in homoleptic products. For instance, the analogous iron(III) complex (**1**)$FeCl_3$ was reported to decompose rapidly into the ion pair [(**1**)$_2$Fe][$FeCl_6$].[40] In the few cases where structural evidence exists for the formation of a heteroleptic (L_{NNN})FeX_2 complex, the *N*-substituent was invariably a secondary alkyl.[41-43] In the case of aromatic *N*-substituents, the presence of *ortho*-substituents is required to prevent the formation of homoleptic ion pairs.[44] Thus, more than 70 solid state structures are reported in the Cambridge Structural database for (L_{NNN})FeX_2 complexes wherein the *N*-substituent is a secondary alkyl or a 2,6-disubstituted aryl,[26] there being no example of such a complex featuring the *N*-substituent as a primary alkyl or an aryl moiety lacking substituents at the 2- and 6-positions. In the absence of such structural evidence, we suspect that several compounds reported as (L_{NNN})FeX_2 with sterically undemanding *N*-substituents might in fact be the ion pairs [(L_{NNN})$_2$Fe][FeX_4].

Complexes with *N*-aryl substituents. In light of the apparent requirement for bulky *N*-substituents to stabilize (L_{NNN})FeX_2, we set out to investigate the accessibility of the analogous heteroleptic complexes (L_{NNN})$Fe(OR)_2$ from authentic halide precursors. We employed for this purpose the previously reported complex {*N,N'*-2,4,6-$Me_3C_6H_2$-bis(imino)pyridine}$FeCl_2$, **9**,[45] which was obtained readily from $FeCl_2$ and the corresponding ligand **8** (Scheme 2.2).[45,46]

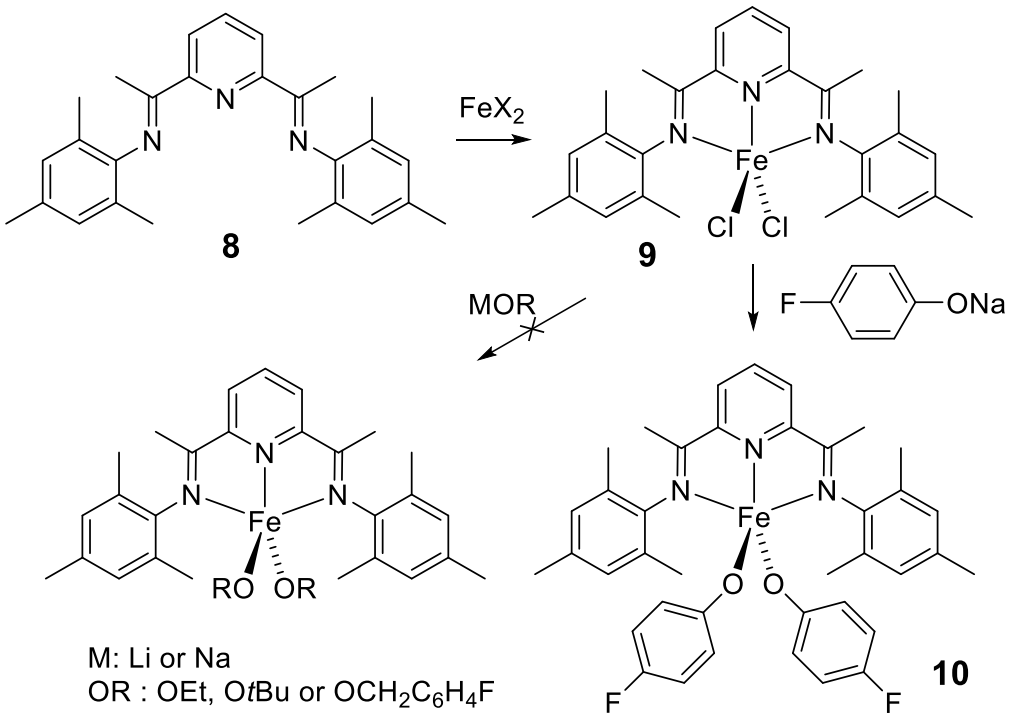

Scheme 2.2

To prepare target $LFe(OR)_2$ species **9** was treated with MOR salts (M= Li, Na; R = Et, *t*-Bu, $CH_2C_6H_4F$, C_6H_4F) in different solvents (THF, CH_2Cl_2, toluene), at several temperatures (–80 to +23 °C), and under a variety of reaction conditions (order of addition, presence of excess MOR, presence of HOR, etc.). Discounting attempts that left the starting materials intact or gave orange-colored decomposition products (also obtained after exposure to air), all reactions proceeded as follows: reaction with MOR led to a gradual dissolution of insoluble **9** and generated a green solution from which was obtained a green, paramagnetic precipitate. Elemental analysis of these green solids did not confirm a heteroleptic bisalkoxide product; ESI-MS was likewise inconclusive. For instance, the mass spectrum of the reaction with NaO*t*Bu featured a minor peak with a

mass corresponding to (**8**)Fe(O*t*Bu)$_2$, but there were a number of other, more intense peaks of both lower and higher mass values.

The failure to identify the green solids prompted us to prepare derivative adducts with xylyl isonitrile and PPh_3. Unfortunately, none of these approaches gave diamagnetic adducts (based on ^{1}H NMR spectra). Strictly speaking however, the failure to generate a diamagnetic, octahedral species cannot be taken as proof against the formation of five-coordinated (**8**)Fe(OR)$_2$ because the precursor complex **9** did not coordinate additional Lewis bases either. UV/vis spectra of the crude green solids (Fig. 2.4) were much more similar to that of **9** than to those of **3-6**, indicating that treatment with MOR did not lead to simple homoleptic species. The latter is unlikely in any case, given the *ortho*-substitution of the phenyl rings in **9** (vide supra). The spectra of all reaction products showed a bathochromic displacement when compared to **9**, consistent with replacement of chloride by OR; the displacement was surprisingly strong for **9**/$NaOC_6H_4F$.

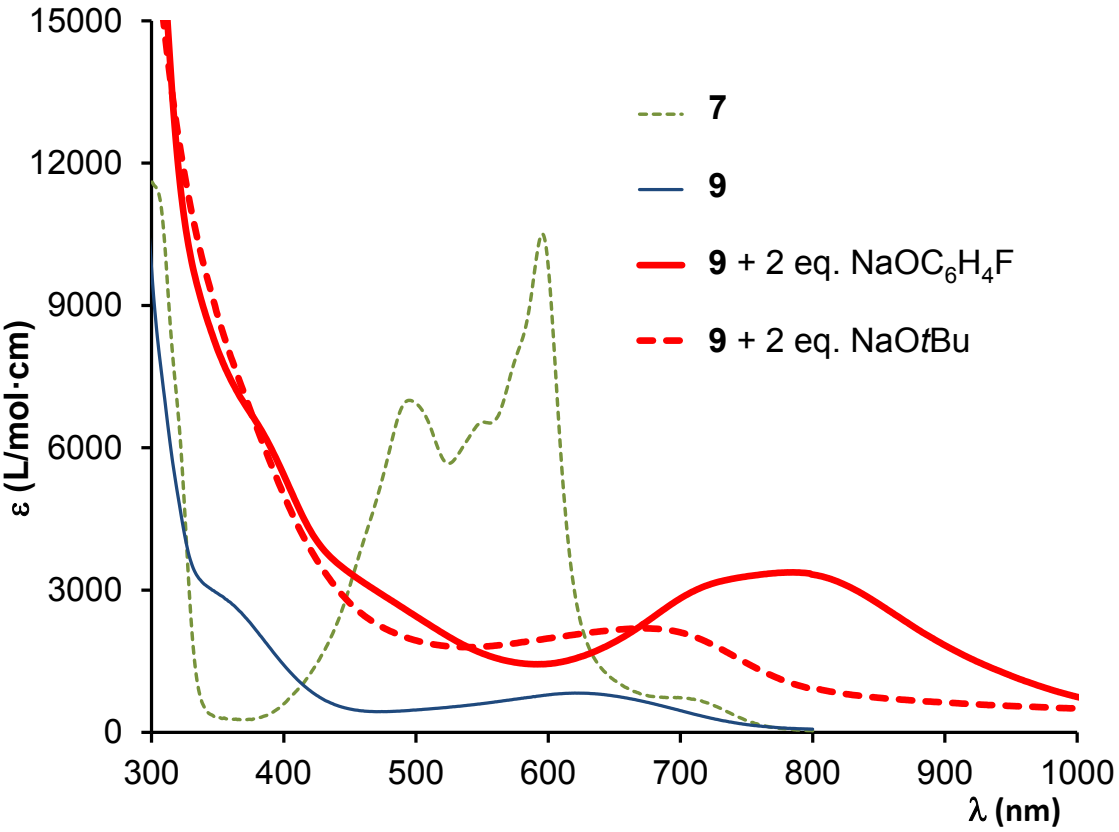

Fig. 2.4: UV/vis spectra of homoleptic complex **7**, heteroleptic **9**, and the green reaction products of **9** + 2 NaOR.

Unfortunately, none of the above synthetic attempts led to an analytically pure alkyl- or aryloxide. In a single, isolated case, recrystallisation of the green product obtained from the reaction of **9** with NaOAr (Ar = *para*-C_6H_4F) yielded a single crystal of the aryloxide derivative (**8**)Fe$(OAr)_2$·ArOH, **10**. X-ray diffraction analysis of this crystal has allowed us to characterize the solid state structure of **10** (Fig. 2.5). Table 2.2 shows a comparison of the structural parameters for **10,** its precursor **9**,[45] and the related complex (**8**)Fe$(OC_6F_5)_2$, which was very recently reported by Cartes *et al*.[47] While bond distances are similar in all complexes, the coordination geometries are somewhat

different. Complexes **9** and (**8**)Fe(OC_6F_5)$_2$ display a trigonal-bipyramidal coordination around iron, while the coordination geometry of **10** is best described as square pyramidal with one phenoxy ligand in the axial position (τ = 0.05).[48] One co-crystallized phenol forms a strong hydrogen bond with the apical phenoxy ligand in **10**. The presence of this solvate is most likely responsible for the decreased Fe1-O1-C30 angle of 128.0(3)°, which is 30° smaller than the respective angle at O2. The Fe-N distances in **10** are slightly shorter than the corresponding distances in **9** or (**8**)Fe(OC_6F_5)$_2$ (Table 2.2). We ascribe this difference to the greater Fe→N backbonding into the diiminopyridine ligand, which is in turn due to the presence of the more electron-rich aryloxy ligand in **10**. Even shorter Fe-N_{py} distances are observed for (**8**)Fe(CH_2SiMe_3)$_2$ (2.006(2) Å)[49] or for the iron(0) complex (L_{NNN})Fe(N_2)$_2$ (1.839(1) Å).[50]

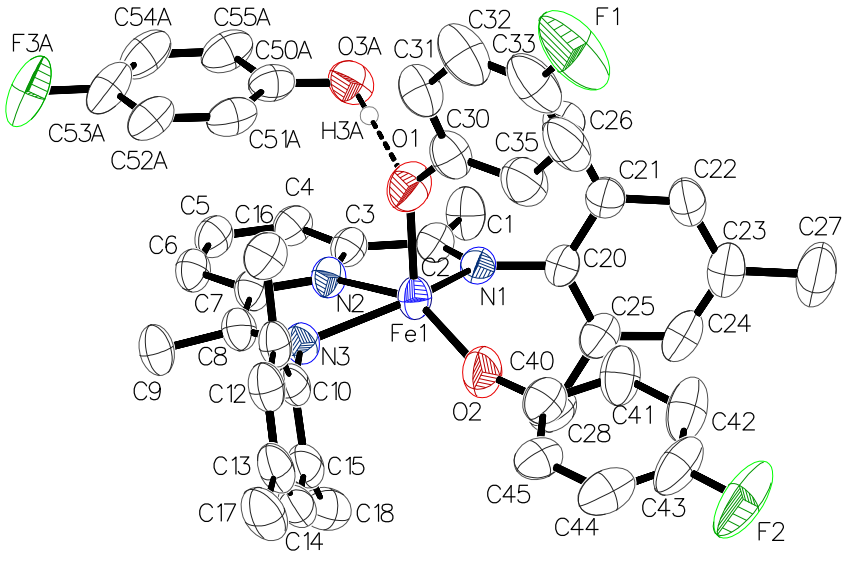

Fig. 2.5: Crystal Structure of **10**. Thermal ellipsoids are drawn at 50% probability. Hydrogen atoms other than H3A, co-crystallized solvent and the minor component of the disordered co-crystallized phenol are omitted for clarity.

Table 2.2: Bond distances (Å) and angles (°) for **10** and related (**8**)FeX_2 complexes.

	10	**9** [a]	(**8**)$Fe(OC_6F_5)_2$ [b]
Fe1-N1, Fe1-N3	2.211(3), 2.234(3)	2.266(6), 2.271(7)	2.237(2), 2.292(2)
Fe1-N2	2.089(3)	2.111(6)	2.094(2)
Fe1-O1	2.022(3)		1.984(1)
Fe1-O2	1.907(3)		1.984(1)
O1-O3A	2.629(8)		
N1-Fe1-N3	144.7(1)	145.5(2)	147.6(1)
X1-Fe1-X2 [c]	119.1(2)	109.8(1)	97.1(1)
X1-Fe-N [c]	93.3(1) - 98.7(1)	96.7(2) – 118.9(2)	98.1(1)- 131.4(1)
X2-Fe1-N2 [c]	147.4(1)	131.2(2)	131.4(1)
Fe1-O1-C30	128.0(3)		135.0(1)
Fe1-O2-C40	159.0(3)		135.0(1)

[a] Taken from ref. [45]. [b] Taken from ref. [47]. [c] X = O (**10**, (**8**)$Fe(OC_6F_5)_2$); X = Cl (**9**).

Elucidation of this solid state structure unequivocally establishes the thermal stability of bis(aryloxide) iron complexes such as **10**. However, despite numerous approaches to growing crystals of other aryloxide derivatives, including ensuring the presence of excess ArOH during crystallization, neither complex **10** nor any derivatives could be obtained in analytically pure form or in yields sufficient for further characterization. While this manuscript was in preparation, Biernesser *et al.* reported that reaction of very similar (L_{NNN})$FeCl_2$ complexes with alkoxide or aryloxide salts does not

lead to any isolable products.[24] These authors report obtaining green compounds via an alternative synthetic approach based on alcoholysis of $(L_{NNN})Fe(CH_2SiMe_3)_2$. These green solids were identified as the anticipated $(L_{NNN})Fe(OAr)_2$ based on mass spectroscopic data and a crystal structure of $[(L_{NNN})Fe(OC_6H_4OMe)_2][PF_6]$, obtained after oxidation, but no elemental analysis or crystal structure analysis was reported for the desired charge-neutral, divalent derivative.

Lactide polymerization. Even though the target complexes $LFe(OR)_2$ could not be isolated in pure form, the observations presented above suggested nevertheless that reaction of **9** with NaOR generates Fe-OR species that might serve our purposes of investigating Fe-promoted polymerization of *rac*-lactide. Thus, we began examining the polymerization activities of species generated in-situ by treating **9** with NaOEt. Addition of two equiv of NaOEt to a THF suspension of **9** and stirring for 15-180 min led to complete dissolution of **9** and concomitant appearance of a green solution, reminiscent of what was observed above. Addition of monomer to the resulting solution brought about the room temperature polymerization of *rac*-lactide (Scheme 2.3). In typical polymerization runs, conversions reached up to 95% after 1 h. A control experiment using NaOEt in the absence of **8** led to reduced polymerization activities (34% conversion after 1 h). More importantly, polymerizations with NaOEt showed time-dependent P_r-values, which declined gradually from 0.65 to 0.45 over a period of 2 h, thus indicating significant transesterification. On the other hand, polymerizations using mixtures of **9**/NaOEt, generally showed random and smaller variations of the P_r-value of ±0.03 over the same time period. These observations argue that the active species is indeed an iron alkoxide complex.

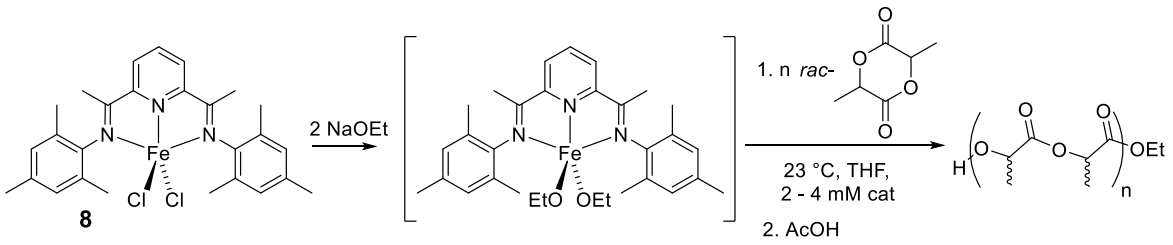

Scheme 2.3

The kinetic profile of the polymerization was independent of the time allowed for the reaction of **9** and NaOEt prior to monomer addition (15 min to 180 min). Similarly, the outcome of polymerization runs was not influenced by minor variations of the **9**:NaOEt ratio (1.9 to 2.1). The observed activities compare well to the ones obtained by Biernesser *et al.* for a presumed $(L_{NNN})Fe(OR)_2$ complex, which was generated by *in-situ* alcoholysis of $(L_{NNN})Fe(CH_2SiMe_3)_2$.[24] In both cases, activities were lower than those of bis(benzimidinate) iron(III) alkoxides,[23] diketiminate iron(II) alkoxides,[22] or anionic ferrous alkoxides $Na_2Fe(OAr)_4(THF)_4$,[51] for which polymerization activity at 70 °C or room temperature was reported.

Unfortunately, **9**/NaOEt did not represent a reliable catalyst system: polymerization yields varied unpredictably and without correlation to reaction conditions. Monitoring of the reaction by sampling and ^{1}H NMR spectroscopy showed that lactide conversions at room temperature varied between 6% and 46% after 1 h of reaction at 2 mM catalyst concentration (8 experiments) and between 23% and >95% at 4 mM catalyst concentration (9 experiments). Even more puzzling and problematic was the finding that none of the polymerization time profiles yielded easily interpretable or reproducible kinetic traces. In all cases, deviations from pure 1st or 2nd order behavior were observed,

and very often a rapid onset of polymerization was followed by a slow growth regime. In several cases, the latter competed with catalyst de-activation, thereby resulting in incomplete final conversions. At the moment, we do not have any indication on the source of catalyst deactivation. The color of the polymerization solution remains a constant green until quenching of the reaction, indicating that decomposition to an orange product, as occasionally observed in the synthetic attempts, does not occur during polymerization. Samples kept for several hours after quenching in reaction solution or in $CDCl_3$ solution afforded results that proved identical to samples processed immediately. This suggests that the above-alluded irreproducible kinetic behavior is not due to post-polymerization modifications arising after the quenching phase, and likely results from variations in catalyst activation, reagent impurities or catalyst instability.

Given the lack of reproducible data, we refrained from further kinetic analyses of the reaction. Table 2.3 presents instead a set of experiments conducted simultaneously with identical batches of catalyst, solvent, and *rac*-lactide to investigate the effects of catalyst and *rac*-lactide concentration. To avoid contamination, no samples were withdrawn for kinetic analysis; instead, the polymerization reactions were quenched after 1 or 12 h of polymerization and the final mixture analyzed. Although conversions of >90% after 1 h have been observed previously in some polymerization trials (*vide supra*), in this set of experiments no reaction reached completion after 12 h. Comparison with the observed conversion after 1 h indicates catalyst decomposition as the possible reason, a scenario further supported by the fact that generally higher final conversions were obtained from reactions at 4 mM vs 2 mM catalyst concentration. Indeed, reactions at 2 mM catalyst concentrations seemed to be somewhat more sensitive to lactide

concentration, with lower conversions noted at lower lactide concentrations. This is in line with the general features of the kinetic profiles described above, i.e., a fast polymerization onset in competition with catalyst deactivation.

It should be added that Biernesser *et al.*[24] have reported a seemingly different polymerization behavior with a comparable $(L_{NNN})Fe(OR)_2$ catalyst: increased conversions were obtained at lower lactide:catalyst ratios. Since in their case lactide concentration was held constant at different lactide:catalyst ratios, however, the increased conversions are probably also related to an increased catalyst concentration.

Table 2.3: *Rac*-lactide polymerization with **9** + 2 NaOEt in THF at ambient temperature (Scheme 2.3)

	[**9**] / mM	**9** : lactide	Reaction time / h	Conversion	P_r [a]	$M_{n,\,GPC}$ / (g/mol) [b]	$M_{w,\,GPC}$ / (g/mol) [b]	M_w/M_n	Polymer chains per Fe centre [c]
#1	2	25	1	44%	0.65				
#2	2	25	12	58%	0.60	<1000			
#3	2	50	1	55%	0.59				
#4	2	50	12	68%	0.60	1500	2300	1.5 [d]	3.2
#5	2	100	1	61%	0.55	3900	5700	1.5	2.2
#6	2	100	12	79%	0.56	5800	8800	1.5	2.0
#7	4	25	1	74%	0.59				
#8	4	25	12	79%	0.58	1300	1900	1.4 [d]	2.2
#9	4	50	1	73%	0.54				
#10	4	50	12	84%	0.55	2100	3800	1.6 [d]	2.9
#11	4	100	1	56%	0.54	2200	4400	2.0 [d]	3.7
#12	4	100	12	87%	0.57	3800	7100	1.9 [d]	3.3

[a] P_r determined from decoupled ^{1}H NMR by $P_r = 2 \cdot I_1/(I_1+I_2)$, with I_1 = 5.20 – 5.25 ppm (*rmr, mmr/rmm*), I_2 = 5.13 – 5.20 ppm (*mmr/rmm, mmm, mrm*). [b] M_n and M_w determined by size exclusion chromatography vs. polystyrene standards, with an MH correction factor of 0.58. [c] determined from (conversion$\cdot m_{lactide}/n_{Fe}+M(EtOH)/M_{n,\,GPC}$. [d] bimodal distribution.

The polymerizations listed in Table 2.3 showed the slight heterotactic bias typically observed for chain-end control in *rac*-lactide polymerization (P_r-values of 0.54 – 0.65). Variations in P_r-values were slightly higher than expected from experimental errors and might indicate the presence of transesterification. This was supported by GPC analyses of the obtained polymers, which showed not only broadened polydispersities (Table 2.3), but also the presence of low molecular weight peaks indicative of intramolecular transesterification to cyclic oligomers. MALDI analyses of selected polymer samples (Fig. 2.6) showed the series of m/z = $n \cdot 144 + M(\text{EtOH}) + M(\text{Na}^+)$ expected for a linear polymer, thus confirming initiation by the ethoxy group. This series also showed varying intensities of peaks at m/z = $(n+0.5) \cdot 144 + M(\text{EtOH}) + M(\text{Na}^+)$, indicative of intermolecular transesterification. A lower intensity series of m/z = $(n) \cdot 72 + M(\text{Na}^+)$ confirmed the presence of cyclic oligomers and thus intramolecular transesterification. Comparison of the consumed mass of lactide per catalyst and the molecular weight of the resulting polymer allows us to calculate the number of chains produced per catalyst. In the absence of chain termination reactions, this would indicate whether one or both alkoxide groups are active in chain growth. The presence of intramolecular transesterification, which increases the number of chains produced per catalyst, renders a clear conclusion difficult in this case. However, MALDI-MS data indicates that polymerizations at 2 mM catalyst concentration display only small amounts of intermolecular transesterification, and the obtained values of 2.0 and 2.3 polymer chains per metal center (Table 2.3, #5 and #6) indicate that both alkoxide groups are active in chain growth.

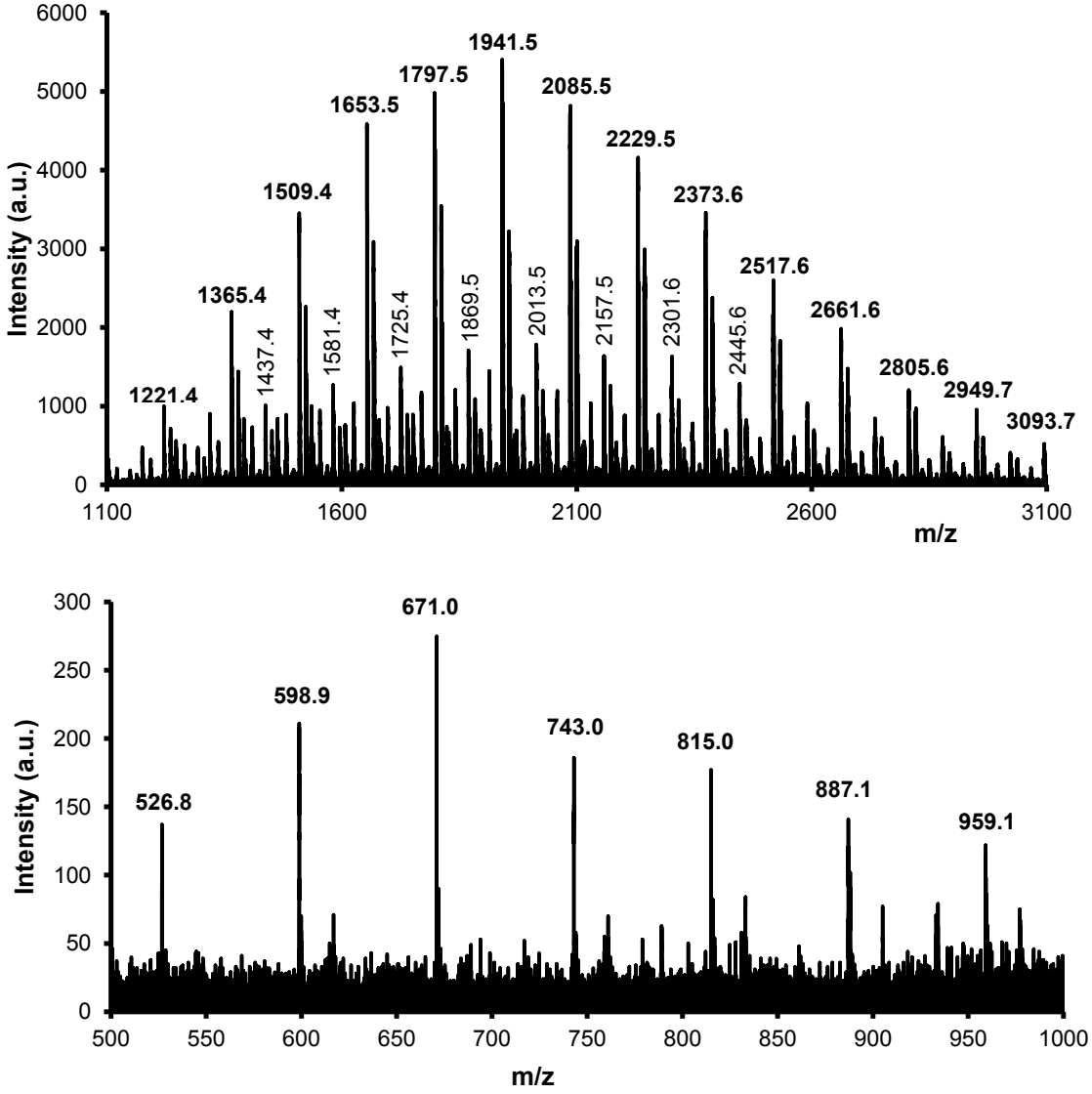

Fig. 2.6: MALDI spectra of PLA obtained with **9**/NaOEt (Table 2.3, #12). Top: $m/z = n \cdot 144 + M(\text{EtOH}) + M(\text{Na}^+)$ in bold, $m/z = (n+0.5) \cdot 144 + M(\text{EtOH}) + M(\text{Na}^+)$ in normal font. Bottom: $m/z = n \cdot 72 + M(\text{Na}^+)$

2.4 Summary

The preparation of iron alkoxide complexes with tridentate diiminopyridine ligands proved more difficult than expected. The use of *N*-benzyl substituted ligands led to sterically saturated, homoleptic, bis(ligand) complexes. This outcome could be avoided with *ortho*-substituted *N*-aryl substituents, but $(L_{NNN})Fe(OR)_2$ or $(L_{NNN})Fe(OAr)_2$ complexes remained elusive despite crystallographic evidence of their formation. The catalytic system **9**/NaOEt was active for the room temperature polymerization of *rac*-lactide. It should be emphasized that this is one of the few iron systems reported for this polymerization, thus showing the potential of iron-based catalysts for this reaction. Unfortunately, however, polymerizations gave unreliable activities, poor molecular weight control and high degrees of transesterification. Isolation of a well-defined iron alkoxide species is required to decide if these side reactions are inherent problems of the catalytic system or consequences of its in-situ formation.

2.5 Experimental Section

General considerations. All reactions involving iron precursors were carried out under a nitrogen atmosphere using Schlenk or glove box techniques. Solvents were dried by passage through activated aluminum oxide (MBraun SPS), de-oxygenated by repeated extraction with nitrogen, and stored over molecular sieves. *rac*-Lactide (98%) was purchased from Sigma–Aldrich, purified by 3x recrystallization from dry ethyl acetate and kept at –30 °C. All other chemicals were purchased from common commercial suppliers and used without further purification. ^{1}H and ^{13}C NMR spectra were acquired

on a Bruker AVX 400 spectrometer. The chemical shifts were referenced to the residual signals of the deuterated solvents (C_6D_6: δ 7.16 (^{1}H), δ 128.4 (^{13}C); $CDCl_3$: δ 7.26 (^{1}H)); coupling constants are expressed in Hz. Elemental analyses were performed by the Laboratoire d'analyse élémentaire (Université de Montréal). Molecular weight analyses were performed on a Waters 1525 gel permeation chromatograph equipped with three Phenomenex columns and a refractive index detector at 35 °C. THF was used as the eluent at a flow rate of 1.0 mL·min^{-1} and polystyrene standards (Sigma–Aldrich, 1.5 mg·mL^{-1}, prepared and filtered (0.2 mm) directly prior to injection) were used for calibration. The molecular weights were corrected by a Mark-Houwink factor of 0.58.[52]

2,6-bis[1-(4-fluorobenzylimino)-ethyl]pyridine, 2. A round bottom flask was charged with 4-fluorobenzylamine (1.97 g, 15.7 mmol) and 2,6-diacetylpyridine (1.00 g, 6.15 mmol), and the resulting mixture was stirred overnight at room temperature. The yellow solid obtained was dissolved in hot anhydrous ethanol, and left to cool to room temperature. After 24 hours, pale yellow crystals were isolated by filtration, washed with cold anhydrous ethanol (3 × 10 mL) and dried under vacuum (1.63 g, 70%).

^{1}H NMR ($CDCl_3$): δ 2.54 (s, 6H, Me), 4.75 (s, 4H, NCH_2), 7.04-7.09 (m, 4H, Ph), 7.41-7.45 (m, 4H, Ph), 7.75 (t, J = 8, 1H, *para* Py), 8.23 (d, J = 8 Hz, 2H, *meta* Py). ^{19}F NMR ($CDCl_3$): δ 116.64 (m). ^{13}C NMR ($CDCl_3$): δ 14.2 (Me), 55.3 (NCH_2), 115.1 (d, J_{CF} = 21, Ar), 121.4 (Ar), 129.1 (d, J_{CF} = 8, Ar), 136.1 (Ar), 136.6 (Ar), 155.8 (Ar), 161.7 (d, J_{CF} = 240), 167.6 (C=N). Anal. Calcd for $C_{23}H_{21}F_2N_3$: C, 73.19; H, 5.61; N, 11.13. Found: C, 73.18; H, 5.63; N, 11.18.

[(1)$_2$Fe][FeCl$_4$]·2(H$_2$O), 3. A suspension of 2,6-bis[1-(benzylimino)-ethyl]pyridine, **1**, (0.69 g, 2.0 mmol) and $FeCl_2$ (0.25 g, 2.0 mmol) in anhydrous THF (30

mL) was stirred overnight at room temperature. Filtration of the final mixture gave a precipitate that was washed with anhydrous THF (3 × 10 mL) and anhydrous diethyl ether (3 × 10 mL), and dried under vacuum to yield a dark purple powder (0.54 g, 56%).

UV–vis (C_2H_5OH, 0.054 mM) [λ_{max}, nm (ε, L/(mol·cm))]: 596 (8800). HRMS (ESI, MeOH) (m/z): $[M]^+$ ($C_{46}H_{46}N_6Fe_2Cl_4$) calcd 936.1214; found 936.1253. $[M-FeCl_4]^{2+}$ ($C_{46}H_{46}N_6Fe$) calcd 369.1562; found 369.1609. Anal. Calcd for $C_{46}H_{46}Cl_4Fe_2N_6 \cdot 2(H_2O)$: C, 56.82; H, 5.18; N, 8.64. Found: C, 56.46; H, 5.24; N, 8.58. (The presence of H_2O confirmed by NMR).

$[(2)_2Fe][FeCl_4]$, 4. Applying the above procedure, **2** (0.39 g, 1.0 mmol), $FeCl_2$ (0.12 g, 0.92 mmol), and anhydrous THF (15 mL) yielded a dark purple powder (0.25 g, 54%).

UV–vis (C_2H_5OH, 0.050 mM) [λ_{max}, nm (ε, L/(mol·cm))]: 596 (8700). HRMS (ESI, MeOH) (m/z): $[M]^+$ ($C_{46}H_{42}F_4N_6Fe_2Cl_4$) calcd 1008.0837; found 1008.0906. $[M-FeCl_4]^{2+}$ ($C_{46}H_{42}F_4N_6Fe$) calcd 405.1373; found 405.1428. Anal. Calcd for $C_{46}H_{42}Cl_4F_4Fe_2N_6$: C, 54.79; H, 4.20; N, 8.33. Found: C, 55.22; H, 4.63; N, 7.80. Crystals for X-ray diffraction were obtained from solvent diffusion of diethyl ether into saturated acetonitrile solution.

$[(1)_2Fe][FeBr_4]\cdot$THF, 5. Applying the above procedure **1**, (0.36 g, 1.1 mmol) and $FeBr_2$ (0.20 g, 0.95 mmol) yielded a dark purple powder (0.25 g, 44%).

UV–vis (C_2H_5OH, 0.046 mM) [λ_{max}, nm (ε, L/(mol·cm))]: 596 (9500). HRMS (ESI, MeOH) (m/z): $[M]^+$ ($C_{46}H_{46}N_6Fe_2Br_4$) calcd 1113.9180; found 1113.9234. $[M-FeBr_4]^{2+}$ ($C_{46}H_{46}N_6Fe$) calcd 369.1562; found 369.1609. Anal. Calcd for

$C_{46}H_{46}Br_4Fe_2N_6 \cdot C_4H_8O$: C, 51.54; H, 4.97; N, 6.68. Found: C, 51.11; H, 4.66; N, 7.18. (The presence of THF confirmed by NMR).

$[(2)_2Fe][FeBr_4] \cdot THF$, 6. Applying the above procedure **2** (0.39 g, 1.0 mmol), $FeBr_2$ (0.20 g, 0.93 mmol), and anhydrous THF (15 mL) yielded a dark purple powder (0.38 g, 65%).

UV–vis (C_2H_5OH, 0.041 mM) [λ_{max}, nm (ε, L/(mol·cm))]: 596 (10200). HRMS (ESI, MeOH) (m/z): $[M]^+$ ($C_{46}H_{42}F_4N_6Fe_2Br_4$) calcd 1185.8803; found 1185.8822. $[M-FeBr_4]^{2+}$ ($C_{46}H_{42}F_4N_6Fe$) calcd 405.1373; found 405.1395. Anal. Calcd for $C_{46}H_{42}Br_4F_4Fe_2N_6 \cdot C_4H_8O$: C, 47.73; H, 4.01; N, 6.68. Found: C, 49.83; H, 4.22; N, 6.89. (The presence of THF confirmed by NMR. EA data indicates the presence of impurities, most likely uncomplexed ligand.)

$[(2)_2Fe][B(Ph)_4]_2$, 7. Adding anhydrous acetonitrile (10 mL) to a mixture of **2** (0.39 g, 1.0 mmol) and $FeCl_2$ (0.63 g, 0.50 mmol) resulted in an immediate colour change to purple. This mixture was stirred for one h at room temperature and then combined with a solution of sodium tetraphenylborate (0.35 g, 1.0 mmol) in acetonitrile (10 mL), and the resulting mixture was allowed to stand overnight at –15 °C. A further portion of sodium tetraphenylborate (0.77 g, 2.2 mmol) in dry ethanol (10 mL) was added to the purple mixture, and the new mixture was left to stand overnight in the refrigerator (ca. 5 °C) to initiate precipitation of final product. Filtration gave a dark purple powder, which was washed with cold dry ethanol (3 × 10 mL) and dried under vacuum to yield the desired product as a dark purple powder (0.66 g, 91%). Compound **7** was recrystallized by

solvent diffusion of diethyl ether into a saturated solution of product in acetonitrile; the obtained crystals were suitable for an X-ray diffraction study.

^{1}H NMR (CD_3CN): δ 2.20 (s, 6H, -CH_3), 3.59 (s, 4H, -NCH_2), 6.25-6.28 (m, 4H), 6.90 (td, J_{HH} = 8, J_{FH} = 14, 8H, Bn), 7.00-7.04 (m, 8H), 7.29-7.31 (m, 8H), 8.36 (d, J_{HH} = 8, 2H, meta Py), 8.55 (t, J_{HH} = 8, 1H, para Py). ^{19}F NMR (CD_3CN): δ 114.76 (m, 2F, para Bn). ^{13}C NMR (CD_3CN): δ 17.4 (Me), 55.8 (NCH_2), 116.6 (d, J_{CF} = 22, Ar), 122.7 (Ar), 126.6 (m, Ar), 127.4 (Ar), 129.1 (d, J_{CF} = 8, Ar), 130.4, 136.6 (Ar), 137.5 (Ar), 161.7 (Ar), 161.8 (Ar), 164-166 (m, Ar), 177.8 (C=N). UV–vis (CH_3CN, 0.032 mM) [λ_{max}, nm (ε, L/ mol·cm)]: 596 (10500). Anal. Calcd for $C_{94}H_{82}B_2F_4FeN_6$: C, 77.90; H, 5.70; N, 5.80. Found: C, 77.35; H, 5.62; N, 5.84.

($C_{27}H_{31}N_3$)$FeCl_2$, 9. A literature procedure was adapted as follows:[45] anhydrous ethanol (15 mL) was added to 2,6-diacetylpyridinebis(2,4,6-trimethylanil) (1.71 g, 4.3 mmol) and $FeCl_2$ (0.49 g, 3.9 mmol) and the resulting mixture was stirred for 15 min at room temperature. Anhydrous diethyl ether was added (50 mL) to precipitate the dark blue product, which was filtered, washed with anhydrous diethyl ether (3 × 15 mL), and dried under vacuum to yield a dark blue powder (1.57 g, 77%). Analytically pure product, used in polymerization experiments, was obtained by recrystallization from a concentrated solution in dichloromethane, layered with an equal amount of hexane (20%).

UV–vis (C_2H_5OH, 0.099 mM) [λ_{max}, nm (ε, L/(mol·cm))]: 620 (540). Anal. Calcd for $C_{27}H_{31}Cl_2FeN_3 \cdot 1.25(CH_2Cl_2)$: C, 53.82; H, 5.36; N, 6.66. Found: C, 53.62; H, 5.28; N, 6.78.

General procedure for lactide polymerization reactions. An 8.0 mM stock solution of **9** in anhydrous THF (1.00 ml) was combined with a 16.0 mM stock solution of sodium ethoxide in anhydrous THF (1.00 ml), and the resulting solution was left stirring for approximately 3 h, whereby the solution developed a dark green colouration. The desired amount of *rac*-lactide was added to the catalyst solution to initiate the polymerization. Stirring was maintained throughout the entire polymerization reaction. An equivalent volume of 24 mM acetic acid in DCM was added to the final reaction mixture to quench the polymerization reaction at the desired time, and the reaction solvent was immediately evaporated under vacuum. Solid polymeric products were stored at -80 °C. Where needed, samples for conversion measurements were obtained throughout the polymerization reaction by taking 100 μl aliquots from the reaction mixture at various times and quenched by adding 100 μl of 24 mM acetic acid in DCM. Aliquot samples were then placed under vacuum to evaporate the solvent. NMR samples were prepared by dissolving solid polymer samples in $CDCl_3$.

X-ray diffraction. Single crystals were obtained as described above. Diffraction data were collected with Cu Kα radiation on Bruker Microstar/Proteum, equipped with Helios mirror optics and rotating anode source or on a Bruker APEXII with a Cu microsource/Quazar MX optics using the APEX2 software package.[53] Data reduction was performed with SAINT,[54] absorption corrections with SADABS.[55] Structures were solved with direct methods (SHELXS97).[56] All non-hydrogen atoms were refined anisotropic using full-matrix least-squares on F^2 and hydrogen atoms refined with fixed isotropic U using a riding model (SHELXL97). Further experimental details can be found in Table 4 and in the supporting information (CIF).

2.6 Acknowledgements

This work was supported by the Natural Sciences and Engineering Research Council of Canada (NSERC) and the Centre in Green Chemistry and Catalysis (CGCC). We thank P. Daneshmand Kashani and Prof. R. E. Prud'homme for GPC analyses, Dr. A. Furtos and M.-C. Tang for mass spectroscopy analyses and Prof. G. Hanan for access to the UV/vis spectrometer.

2.7 Supporting Information

Details of the X-ray diffraction studies (CIF).

Table 2.4: Details of X-ray Diffraction Studies

		[(**2**)$_2$Fe][Cl_6Fe_2O]	**7**	**10**	$Na_4Fe_2(OC_6H_4F)_8$
Formula		[$C_{46}H_{42}F_4FeN_6$][Cl_6Fe_2O]	[$C_{46}H_{42}F_4FeN_6$][2 $C_{24}H_{20}B$] · 4 C_2H_3N	$C_{45}H_{39}F_2FeN_3O_2$· C_6H_5FO·C_7H_8	$C_{28}H_{24}F_4FeNa_2O_5$
M_w (g/mol); $d_{calcd.}$ (g/cm^3)		1151.10; 1.492	1613.34; 1.256	879.81; 1.289	618.30; 1.493
T (K); F(000)		150; 2336	100; 3392	100; 1848	150; 632
Crystal System		Monoclinic	Monoclinic	Orthorhombic	Triclinic
Space Group		$P2_1/n$	$C2/c$	$P2_12_12_1$	P–1
Unit Cell:	a (Å)	11.9682(4)	23.3366(8)	15.1071(3)	10.7568(5)
	b (Å)	20.6810(8)	14.2139(5)	16.8231(3)	11.2080(6)

c (Å)	21.4694(8)	27.9747(10)	17.8423(3)	13.7636(8)
α (°)				92.791(3)
β (°)	105.375(2)	113.134(2)		108.246(2)
γ (°)				116.486(2)
V (Å^3); Z	5123.8(3); 4	8533.2(5); 4	4534.6(1);4	1375.5(1); 2
μ (mm^{-1}); Abs. Corr.	10.066; multi-scan	1.924; multi-scan	3.143; multi-scan	5.282; multi-scan
θ range (°); completeness	3.0 – 67.7; 1.00	3.7 – 67.7; 1.00	3.6 – 67.7; 1.00	3.5 – 70.4; 0.97
collected reflections; R_σ	122970; 0.023	82554; 0.020	87007; 0.034	48601; 0.040
unique reflections; R_{int}	9595; 0.052	8193; 0.041	8579; 0.038	5097; 0.074
R1(F) ($I > 2\sigma(I)$)	0.036	0.041	0.048	0.062
wR(F^2) (all data)	0.096	0.114	0.142	0.190
GoF(F^2)	1.07	1.05	1.06	1.05
Residual electron density	0.53; –0.33	0.56; –0.40	0.44, –0.27	0.89, –0.63

2.8 References

(1) Vink, E. T. H.; Rábago, K. R.; Glassner, D. A.; Springs, B.; O'Connor, R. P.; Kolstad, J.; Gruber, P. R. *Macromol. Biosci.* **2004**, *4*, 551.

(2) Ahmed, J.; Varshney, S. K. *Int. J. Food Prop.* **2011**, *14*, 37.

(3) Inkinen, S.; Hakkarainen, M.; Albertsson, A.-C.; Södergård, A. *Biomacromolecules* **2011**, *12*, 523.

(4) Slomkowski, S.; Penczek, S.; Duda, A. *Polymers for Advanced Technologies* **2014**, *25*, 436.

(5) Wheaton, C. A.; Hayes, P. G.; Ireland, B. J. *Dalton Trans.* **2009**, 4832

(6) Ajellal, N.; Carpentier, J.-F.; Guillaume, C.; Guillaume, S. M.; Helou, M.; Poirier, V.; Sarazin, Y.; Trifonov, A. *Dalton Trans.* **2010**, *39*, 8363.

(7) Sutar, A. K.; Maharana, T.; Dutta, S.; Chen, C.-T.; Lin, C.-C. *Chem. Soc. Rev.* **2010**, *39*, 1724.

(8) Buchard, A.; Bakewell, C.; Weiner, J.; Williams, C. In *Organometallics and Renewables*, Meier, M. A. R.; Weckhuysen, B. M.; Bruijnincx, P. C. A., Eds. Springer Berlin Heidelberg: 2012; Vol. 39, pp 175.

(9) dos Santos Vieira, I.; Herres-Pawlis, S. *Eur. J. Inorg. Chem.* **2012**, *2012*, 765.

(10) Dean, R. K.; Reckling, A. M.; Chen, H.; Dawe, L. N.; Schneider, C. M.; Kozak, C. M. *Dalton Trans.* **2013**, *42*, 3504.

(11) Sauer, A.; Kapelski, A.; Fliedel, C.; Dagorne, S.; Kol, M.; Okuda, J. *Dalton Trans.* **2013**, *42*, 9007.

(12) Dagorne, S.; Normand, M.; Kirillov, E.; Carpentier, J.-F. *Coord. Chem. Rev.* **2013**, *257*, 1869.

(13) Jianming, R.; Anguo, X.; Hongwei, W.; Hailin, Y. *Des. Monomers Polym.* **2013**, *17*, 345.

(14) Aluthge, D. C.; Yan, E. X.; Ahn, J. M.; Mehrkhodavandi, P. *Inorg. Chem.* **2014**, *53*, 6828.

(15) Chamberlain, B. M.; Cheng, M.; Moore, D. R.; Ovitt, T. M.; Lobkovsky, E. B.; Coates, G. W. *J. Am. Chem. Soc.* **2001**, *123*, 3229.

(16) Whitehorne, T. J. J.; Schaper, F. *Chem. Commun. (Cambridge, U. K.)* **2012**, *48*, 10334.

(17) Whitehorne, T. J. J.; Schaper, F. *Inorg. Chem.* **2013**, *52*, 13612.

(18) Whitehorne, T. J. J.; Schaper, F. *Can. J. Chem.* **2014**, *92*, 206.

(19) Kricheldorf, H. R.; Damrau, D.-O. *J. Macromol. Sci., Part A: Pure Appl.Chem.* **1998**, *35*, 1875.

(20) Idage, B. B.; Idage, S. B.; Kasegaonkar, A. S.; Jadhav, R. V. *Mater. Sci. Eng., B* **2010**, *168*, 193.

(21) Rajashekhar, B.; Chakraborty, D. *Polym. Bull.* **2014**, *71*, 2185.

(22) Gibson, V. C.; Marshall, E. L.; Navarro-Llobet, D.; White, A. J. P.; Williams, D. J. *J. Chem. Soc., Dalton Trans.* **2002**, 4321.

(23) O'Keefe, B. J.; Breyfogle, L. E.; Hillmyer, M. A.; Tolman, W. B. *J. Am. Chem. Soc.* **2002**, *124*, 4384.

(24) Biernesser, A. B.; Li, B.; Byers, J. A. *J. Am. Chem. Soc.* **2013**, *135*, 16553.

(25) Manna, C. M.; Kaplan, H. Z.; Li, B.; Byers, J. A. *Polyhedron* **2014**, *84*, 160.

(26) Allen, F. H. *Acta Crystallogr., Sect. B: Struct. Sci.* **2002**, *B58*, 380.

(27) de Bruin, B.; Bill, E.; Bothe, E.; Weyhermüller, T.; Wieghardt, K. *Inorg. Chem.* **2000**, *39*, 2936.

(28) Chen, R.-F.; Qian, C.-T.; Sun, J. *Chin. J. Chem.* **2001**, *19*, 866.

(29) Chen, Y.; Qian, C.; Sun, J. *Private communication to the Cambridge Structural Database* **2004**, CCDC 190475.

(30) Chen, Y.; Qian, C.; Sun, J. *Private communication to the Cambridge Structural Database* **2004**, CCDC 190476.

(31) Britovsek, G. J. P.; England, J.; Spitzmesser, S. K.; White, A. J. P.; Williams, D. J. *Dalton Trans.* **2005**, 945.

(32) Bart, S. C.; Bowman, A. C.; Lobkovsky, E.; Chirik, P. J. *J. Am. Chem. Soc.* **2007**, *129*, 7212.

(33) Trovitch, R. J.; Lobkovsky, E.; Bouwkamp, M. W.; Chirik, P. J. *Organometallics* **2008**, *27*, 6264.

(34) Wile, B. M.; Trovitch, R. J.; Bart, S. C.; Tondreau, A. M.; Lobkovsky, E.; Milsmann, C.; Bill, E.; Wieghardt, K.; Chirik, P. J. *Inorg. Chem.* **2008**, *48*, 4190.

(35) Badiei, Y. M.; Siegler, M. A.; Goldberg, D. P. *J. Am. Chem. Soc.* **2011**, *133*, 1274.

(36) Gong, D.; Jia, X.; Wang, B.; Wang, F.; Zhang, C.; Zhang, X.; Jiang, L.; Dong, W. *Inorg. Chim. Acta* **2011**, *373*, 47.

(37) Furlani, C.; Cervone, E.; Valenti, V. *J. Inorg. Nucl. Chem.* **1963**, *25*, 159.

(38) Forster, D.; Goodgame, D. M. L. *J. Chem. Soc.* **1965**, 454.

(39) Lappalainen, K.; Yliheikkilä, K.; Abu-Surrah, A. S.; Polamo, M.; Leskelä, M.; Repo, T. *Z. Anorg. Allg. Chem.* **2005**, *631*, 763.

(40) Görl, C.; Englmann, T.; Alt, H. G. *Appl. Catal., A* **2011**, *403*, 25.

(41) Castro, P. M.; Lappalainen, K.; Ahlgrén, M.; Leskelä, M.; Repo, T. *J. Polym. Sci., Part A: Polym. Chem.* **2003**, *41*, 1380.

(42) Pelascini, F.; Wesolek, M.; Peruch, F.; Lutz, P. J. *Eur. J. Inorg. Chem.* **2006**, *2006*, 4309.

(43) Tondreau, A. M.; Lobkovsky, E.; Chirik, P. J. *Org. Lett.* **2008**, *10*, 2789.

(44) Ionkin, A. S.; Marshall, W. J.; Adelman, D. J.; Fones, B. B.; Fish, B. M.; Schiffhauer, M. F. *Organometallics* **2006**, *25*, 2978.

(45) Britovsek, G. J. P.; Bruce, M.; Gibson, V. C.; Kimberley, B. S.; Maddox, P. J.; Mastroianni, S.; McTavish, S. J.; Redshaw, C.; Solan, G. A.; Strömberg, S.; White, A. J. P.; Williams, D. J. *J. Am. Chem. Soc.* **1999**, *121*, 8728.

(46) A crystal structure of this ligand was submitted to the Cambridge Structural Database: B. Mougang-Soume, A. Keuguerian, D. Zargarian, F. Schaper, 2014, CCDC 1035787.

(47) Ángeles Cartes, M.; Palma, P.; Sandoval, J. J.; Cámpora, J.; Álvarez, E. *Inorg. Chim. Acta* **2014**, *412*, 73.

(48) Addison, A. W.; Rao, T. N.; Reedijk, J.; van Rijn, J.; Verschoor, G. C. *J. Chem. Soc., Dalton Trans.* **1984**, 1349.

(49) Cámpora, J.; Naz, A. M.; Palma, P.; Álvarez, E.; Reyes, M. L. *Organometallics* **2005**, *24*, 4878.

(50) Russell, S. K.; Darmon, J. M.; Lobkovsky, E.; Chirik, P. J. *Inorg. Chem.* **2010**, *49*, 2782.

(51) McGuinness, D. S.; Marshall, E. L.; Gibson, V. C.; Steed, J. W. *J. Polym. Sci., Part A: Polym. Chem.* **2003**, *41*, 3798.

(52) Save, M.; Schappacher, M.; Soum, A. *Macromol. Chem. Phys.* **2002**, *203*, 889.

(53) *APEX2*, Release 2.1-0; Bruker AXS Inc.: Madison, USA, 2006.

(54) *SAINT*, Release 7.34A; Bruker AXS Inc.: Madison, USA, 2006.

(55) Sheldrick, G. M. *SADABS*, Bruker AXS Inc.: Madison, USA, 1996 & 2004.

(56) Sheldrick, G. M. *Acta Crystallogr.* **2008**, *A64*, 112.

Chapter 3

Additional Experiments

3.1 Iron alkoxide synthesis and ligand metathesis reactions

As explained and demonstrated in the previous chapter, the reaction between iron (II) dichlorides or dibromides with tridentate *N*-benzyl ligands, which had been obtained by condensation of bis(acetyl) pyridine with benzyl amines, brought about the formation of the corresponding homoleptic $[L_2Fe][FeX_4]$ ion-pair species. Upon proper characterization of these homoleptic complexes, the preparation of the corresponding heteroleptic $(L)Fe(OR)_2$ complexes was attempted, by treating the ion-pair species with two or more equivalents of sodium ethoxide or aryl oxide salts. However, these attempts did not lead to any isolable product, apart from a single crystal that turned out to be a sodium-iron cluster obtained through the treatment of a homoleptic ion-pair complex with excess sodium fluoro-aryl oxide salt.

It is noteworthy, however, to mention the various synthetic routes and schemes that were attempted within the framework of these endeavors. Considerable effort was first directed into breaking the bis-ligand homoleptic iron (II) complex via coordination of the latter with highly sigma-donating ligands, such as xylyl isocyanide. The possibility of producing a neutral 6-coordinate iron (II) dichloride 18 electron complex was thereby envisaged, and would have been particularly interesting since such a product would also be a diamagnetic species, and the appearance of such a compound would have been apparent through NMR spectroscopy. However, no product was observed through such a coordination reaction, either by NMR, or by

the disappearance of the characteristic deep purple color of the homoleptic ion-pair iron (II) complex in the reaction mixture.

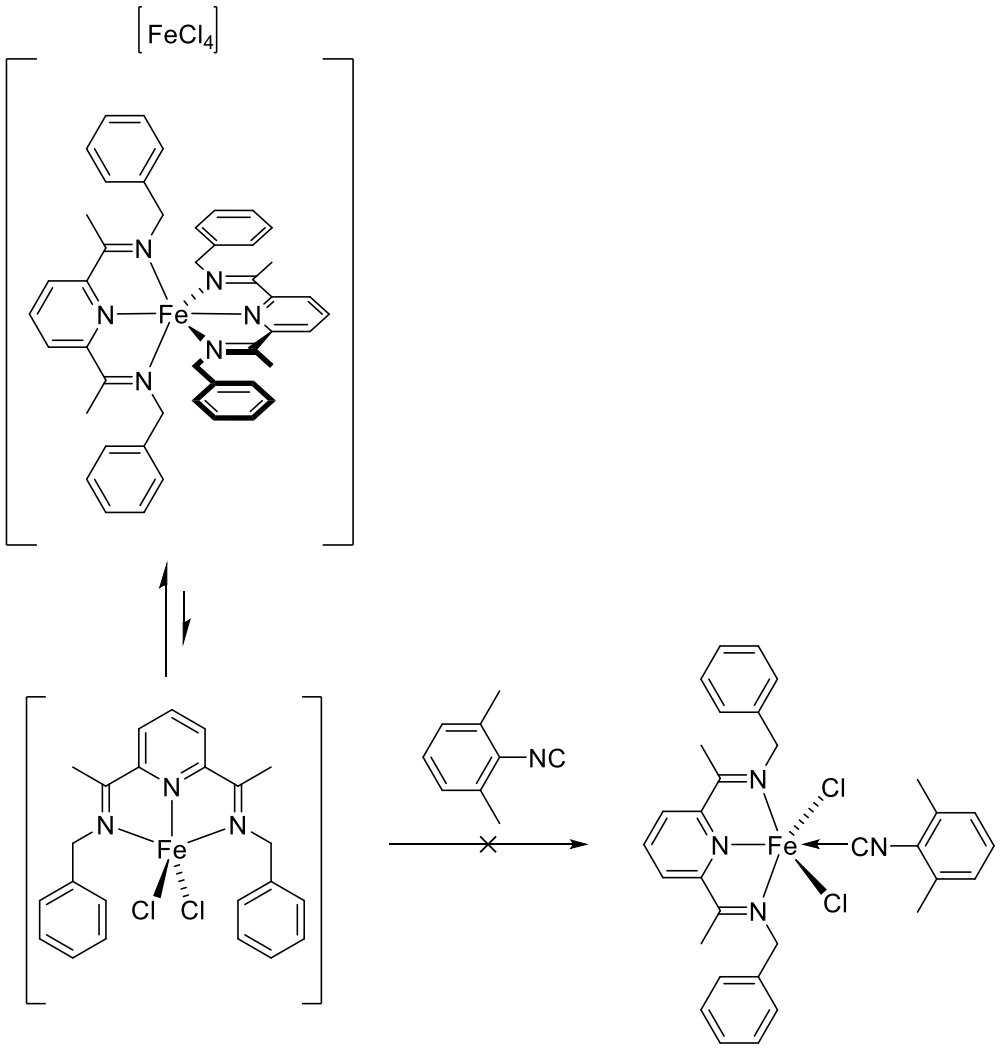

Scheme 3.1: Coordination of xylyl isocyanide to iron (II) dichloride complex

Further variations were also attempted within the ligand coordination reaction itself, and thereby within the synthetic methodology of the homoleptic ion pair complexes. These changes

were made with respect to the reaction solvent and temperature, with the hopes that such variations would bring about the formation of the $(L)Fe(OR)_2$ complex, and allow the isolation of the heteroleptic product before the formation of the homoleptic product via any bimolecular ligand exchange reaction. These attempts encompassed changing the reaction solvent to diethyl ether, acetonitrile, pyridine and even toluene. These variations were generally attempted with the expectation that the heteroleptic product would precipitate before a ligand exchange reaction could occur. In the case of pyridine and acetonitrile, the attempts were carried out with the expectation of creating coordinative saturation at the iron (II) center, so as to promote the stability and isolation of the heteroleptic species. Unfortunately, none of these attempts resulted in the isolation of such a product. The homoleptic ion-pair species was produced in the case of all these reaction attempts, with the appearance of its characteristic deep purple coloration.

In view of the above mentioned experiments, as well as the results presented in the previous chapter, further investigations into the synthesis of iron (II) alkoxide species were carried out with the use of *N*-aryl substituted bis(imino) pyridine ligands. The preparation of heteroleptic $(L)FeX_2$ (L = *N,N*'-dimesityldiiminopyridine), **2.9** was performed according to literature, upon which salt metathesis reactions were attempted with various alkoxide and aryl oxide salts, in different solvents, and at various temperatures. The general scheme and experimental procedure of these reactions are presented in Chapter 2 of this manuscript. As mentioned in the latter, all these reactions led to the gradual dissolution of the bis(imino) pyridine iron (II) dichloride complex, and generated a green solution, from which a green paramagnetic solid product could be obtained.

The previous chapter adequately demonstrates the failure in isolating pure samples and properly characterizing these solid green products, apart from high-resolution MS evidence, and

a single crystal that confirmed the formation and the five-coordinate geometry of the desired bis(imino) pyridine iron (II) bis-aryloxide complex. It is worth mentioning, however, that a great number of crystallization and recrystallization experiments were carried out on each and every one of these reaction products, with variations in solvents, temperatures, as well as methodology, between solvent diffusion through gas phase and liquid phase. However, none of these attempts resulted in crystalline or pure material. Since the crystal structure of **2.10**, the only obtained evidence for a heteroleptic aryl oxide complex, contained a co-crystallized, hydrogen-bonded para-fluoro phenol, we suspected that its presence might either enable crystallization or facilitate preparation of the heteroleptic complex. Preparation or recrystallization of **2.10** was thus attempted in the presence of different amounts of excess phenol, but – again – no crystalline material was obtained and – where analyzed – the obtained powders showed unsatisfactory elemental analysis.

In an attempt to optimize reaction conditions with model complexes, the reaction of **2.9** with alkaline salts of thiocyanate, benzoate, phthalimide, or hydroxyphthalimide were undertaken. However, once again, pure samples and properly characterized products could not be obtained in any of these reactions.

3.2 Lactide Polymerization

Chapter 2 of this manuscript described the experimental procedures, analytical methodology and results of the lactide polymerization reactions with an in-situ produced bis(imino) pyridine iron bis-alkoxide complex as a catalyst. The initial objective was the

compilation of a kinetic data, i.e. concentration vs. time profiles to characterize this type of catalyst.

Table 3.1 provides a summary of nearly all reactions that were not included in the results section of the previous chapter. The table omits a small number of reactions which were done as preliminary work to the project, with the purpose of adjusting the general experimental procedure of the lactide polymerization reactions, and which included very little kinetic profiling data.

As mentioned before, the resulting polymerization yields varied without any direct correlation to the reaction conditions. For example:

- Conversion after 1 h reaction time under identical conditions varied between 6% and 46% (runs 3-6).
- No difference between 1:25 and 1:50 catalyst/lactide ratios at 2 mM catalyst concentration (runs 8-12), but a strong difference at 4 mM catalyst ratio (runs 14-21).
- Reactions with the second batch of catalyst (runs 14-17) show slightly lower activity than those with the first batch under identical conditions (runs 13&14), but runs 18-21 using also the second batch of catalyst show the highest activities of all experiments.
- The high catalytic activities (runs 18-21) could not be reproduced in the reactions in Chapter 2, despite identical reagent batches and reaction conditions.

Table 3.1: Lactide polymerization kinetic experiments

Run	[**2.9**]/2 NaOEt	[lactide]:[cat.]	Conversion after 1 hour	Final conversion	
#	mM	equivalents	%	Time (hours)	%
0	2	100 (no NaOEt)		2	9
1	0	100:2 NaOEt	35	2	44
2	0	100:2 NaOEt	91	4	92
3	2	100	26	2	52
4	2	100	23	4	46
5	2	100	46	7	62
6	2	100	30	9	47
7	2	100	6	9	4
8	2	50	32	2	48
9	2	50	30	2	42
10	2	25	34	2	45
11	2	25	28	2	41
12	4	50	55	2	70
13	4	50	63	2	63
14	4	50	26	3	43
15	4	50	25	3	45
16	4	50	24	3	43
17	4	50	23	3	40
18	4	25	91	24	96
19	4	25	94	24	97
20	4	25	91	24	97
21	4	25	97	24	98

Only one batch of lactide was used throughout these experiments. The same batch of lactide has been employed after the end of the experimental work by Todd Whitehorne in polymerizations using a copper catalyst and yielded the expected reactivities. Lactide impurities or degradation can thus be excluded. Only two different batches of bis(imino) pyridine iron dichloride complex were used throughout all these experiments in runs #1 to #13 and runs #14 to #21, respectively. Both batches were prepared according to the same experimental procedure, in terms of both synthesis and recrystallization and purification. The elemental analysis of the second batch was in complete agreement with the calculated data (see Chapter 2, experimental part).

The iron dichloride precursor complex without addition of NaOEt (run 1) provided hardly any catalytic activity, reaching no more than 9% lactide conversion results after more than 2 h. However, very surprisingly, sodium ethoxide appeared to furnish a very high catalytic activity indeed. Table 1 reports two of these reactions, where conversions of 44% and 92% were reached after 2 to 4 h of reaction. Other NaOEt-catalyzed polymerizations (Chapter 2) also produced lactide conversion results of more than 90% after only two hours. NaOEt is however unlikely to be the active catalytic species in the presence of iron complex **2.9** for reasons discussed in Chapter 2.

Even more worrisome, the time-dependent lactide conversion results of these reactions did not yield any interpretable or reproducible profiles. Figure 3.1 presents the time dependent lactide polymerization conversions with the in-situ produced iron catalyst complex (Run #4), as well as for a blank reaction with only sodium ethanolate present in solution (Run #3).

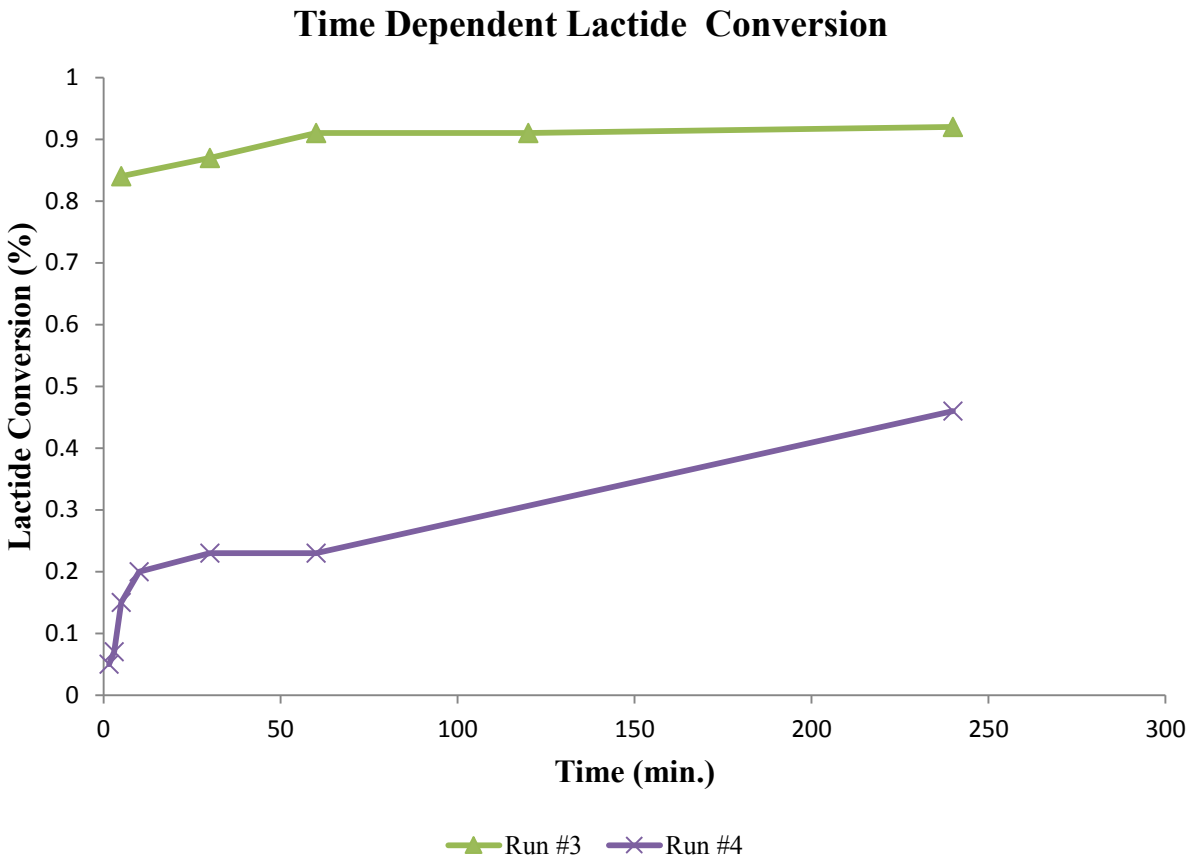

Fig. 3.1: Time dependent lactide conversions for runs #3 and #4.

Not only can one observe, in the above figure, the very active catalytic activity of sodium ethoxide, but also the irregular lactide conversion rate with the iron catalyst system. Fast initial reactivity is followed by deactivation to a slow growth regime. An intuitive interpretation of this concentration-time profile would be that NaOEt is the catalytic species, slowly consumed by **2.9** to form an unreactive iron alkoxide complex. Several experiments (described in Chapter 2) were undertaken to exclude this possibility:

- Reaction time between NaOEt and **2.9** before addition of lactide was varied between 15 min and 2 h without any noticeable impact on conversion.
- Variations of the amount of NaOEt added (1.9 – 2.1 equivalents) also did not have any impact on the observed conversion.
- Polymer properties differ between polymers obtained from NaOEt and **2.9**/NaOEt.

Figure 3.2 shows two reactions that were carried out in exactly the same conditions, with 2 mM of iron catalyst and with 100 equivalents of lactide in solution, with the exact same reagent batches and solutions, and with the exact same experimental procedure.

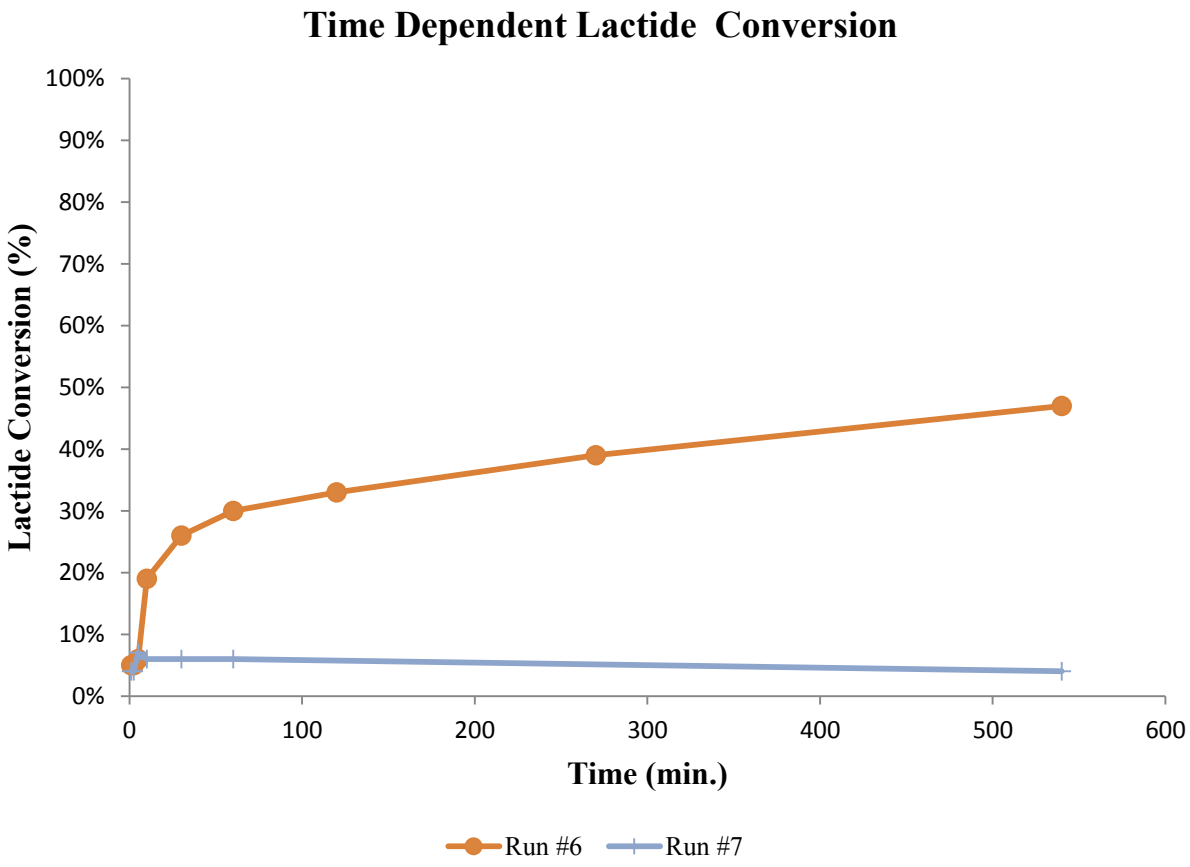

Fig. 3.2: Time dependent lactide conversions for runs #6 and #7.

A re-occurring feature observed in most conversion/time profiles is a measurable conversion even after a few minutes, which seem to remain constant. This is followed by a fast onset of polymerization and deactivation to a slow growth or no-growth regime. Numerous tests were carried out to verify if the constant conversion observed in the first minutes might be an artefact from our analytical methods (i. e. post-quenching polymerization). Tests were thus carried out with respect to how long the reaction aliquot samples were left in solution after being added to the quenching acetic acid solution, before stripping off the solvent for these samples. Two identical aliquots were taken and quenched at the same time, whereby one was placed under vacuum immediately, whereas the other was left in solution for more than two hours before evaporation of the solvent. Both samples showed identical conversion results and there is thus no polymerization after quenching of the catalyst. .

Likewise NMR data on aliquot samples were again recorded after leaving said samples on the bench for more than a day. Again, no change in conversion was obtained, thus there is no conversion (or depolymerization) in the NMR tube either.

Despite the inconclusive nature of the polymerization results, time-dependent concentration profiles were nevertheless recorded at different catalyst and lactide concentrations. In the first place, lactide concentrations were varied from 100 equivalents, as shown in the previous figures, to 50 or 25 equivalents of lactide with respect to iron catalyst. Figure 3.3 presents the time-dependent lactide conversion results for these polymerization reactions with 50 equivalents (Runs #8 and #9) and 25 equivalents (Runs #10 and #11) of lactide. Similarly to the polymerization reactions using 100 equivalents of lactide to catalyst ratio, the results for these

reactions did not reach more than 50% conversion after 2 hours. The kinetic profile for these reactions did not follow any interpretable kinetic order; reactions all seem to start at a very high rate, reaching already 20% after only 5 minutes, and presented a continuous and almost linear growth afterwards.

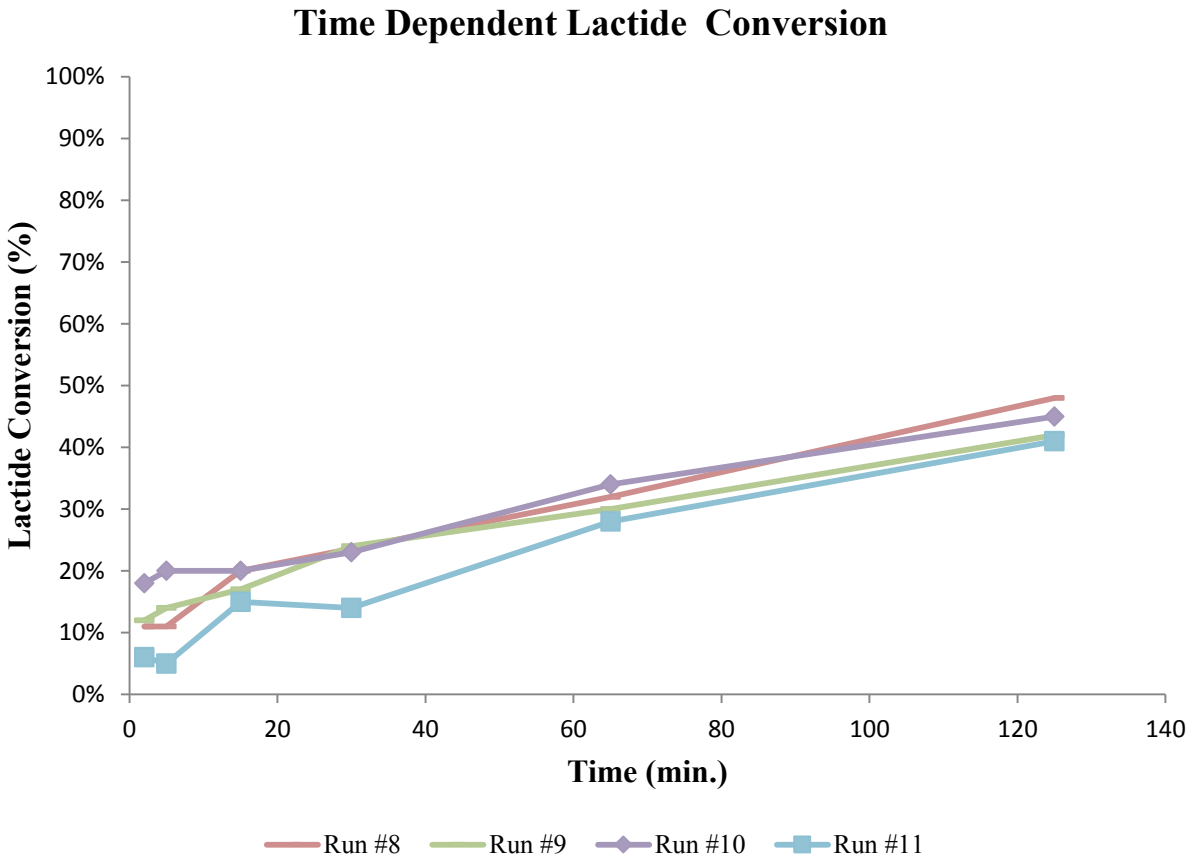

Fig. 3.3: Time dependent lactide conversions for runs #8, #9, #10 and #11.

Following up on these results, catalyst concentrations were also varied and increased from 2 mM to 4 mM.. Figure 3.4 displays the time-dependent lactide conversion results for

reactions with 50 equivalents of lactide to catalyst ratio, with catalyst concentrations of 2 mM (Runs #8 and #9) and of 4 mM (Runs #12 and #13). The expected net increase in polymerization conversion with increase of catalyst concentrations can be clearly observed. However, Fig. 3.4 also displays the irregular kinetic scheme of these polymerization reactions described above.

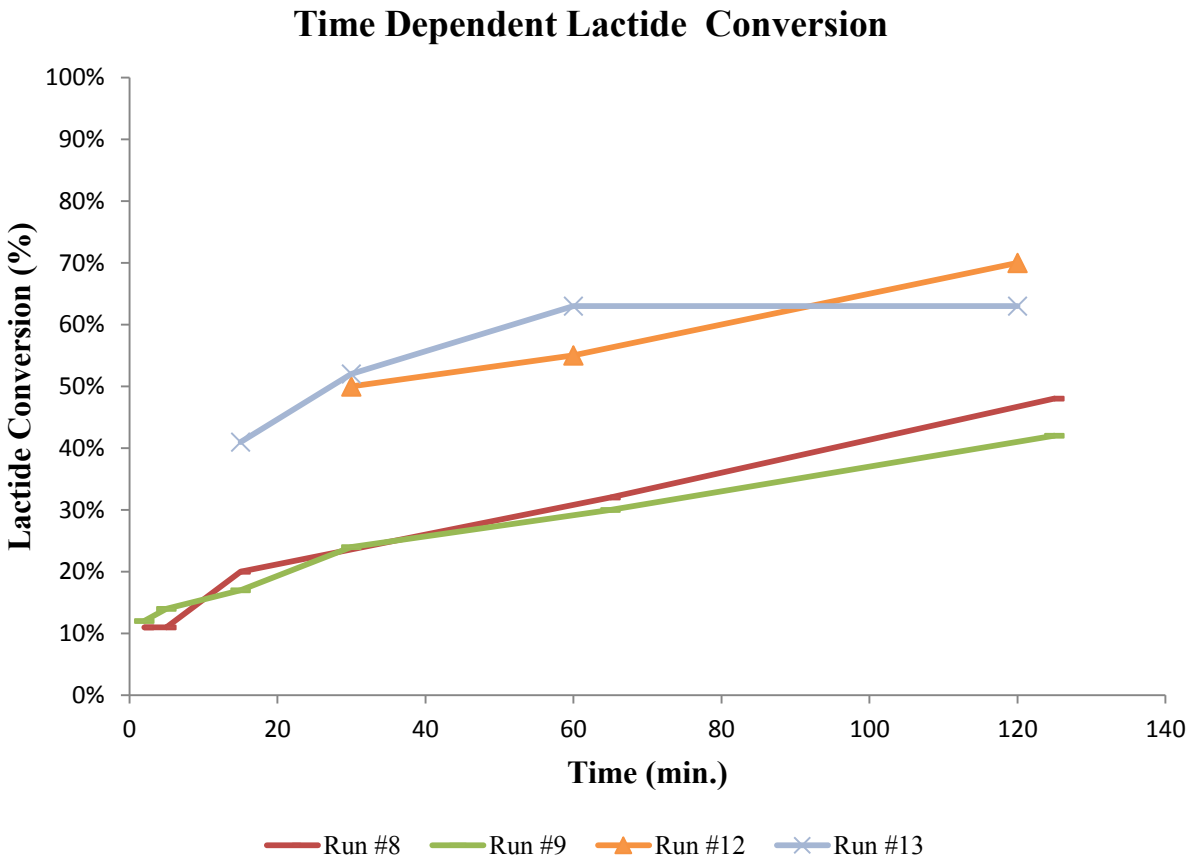

Fig. 3.4: Time dependent lactide conversions for runs #8, #9, #12 and #13.

In order to investigate these kinetic problems, a particular effort was given to getting conversion results within the first 5 to 10 minutes of the reaction, in order to observe exactly what happens at the very onset of the reaction, and before conversion above 20% could be

reached. The following figure presents the first two hours for Runs #18 to #21, where lactide conversion data points were obtained at 0, 1, 2, 5, 15, 30 and 60 minutes. However, for reasons which we were not able to elucidate, in the case of all four reactions, several aliquot samples that were taken between 5 and 60 minutes did **not produce any distinguishable NMR data for analysis**, even though they were collected using the same experimental procedure. Their NMR spectra only showed noisy baselines and indistinguishable signals, characteristic of paramagnetic species. It should be noted that these four experiments were not performed at the same day.

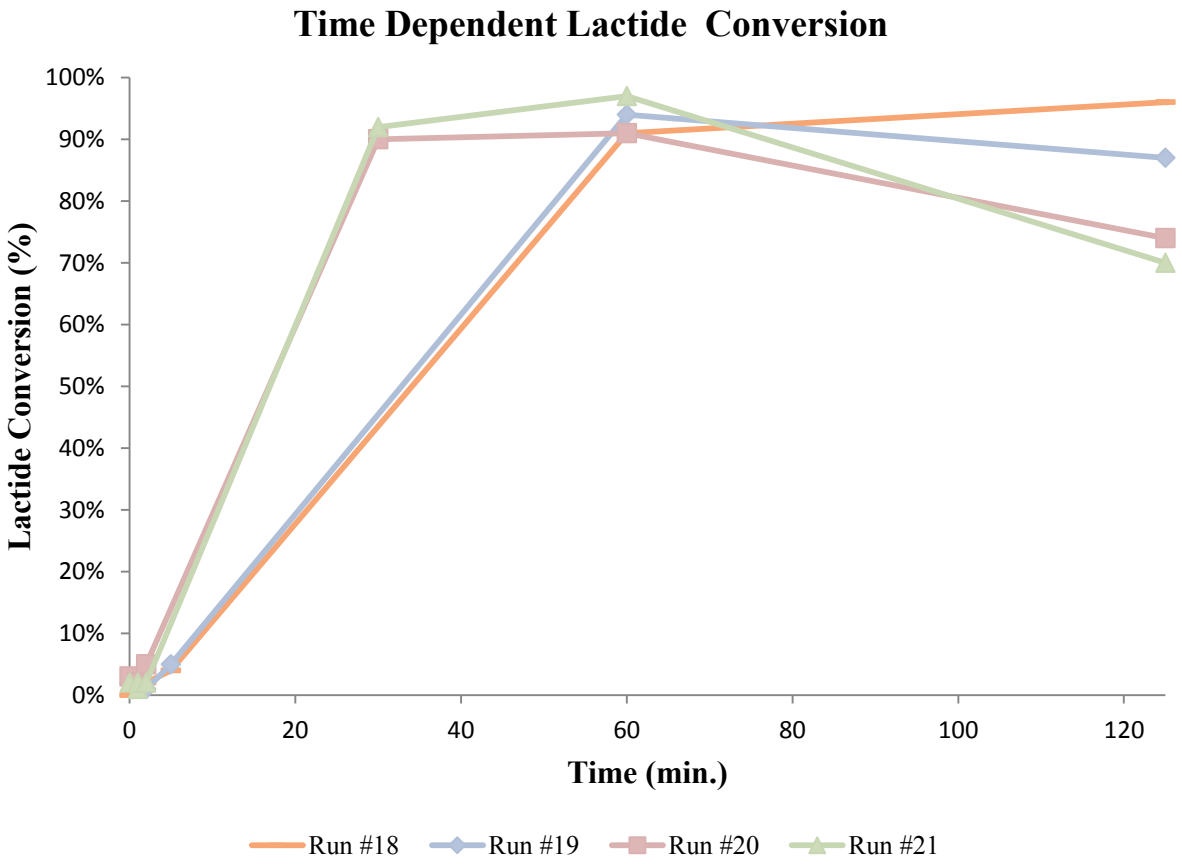

Fig. 3.5: Time dependent lactide conversions for runs #18, #19, #20 and #21.

All these results, or more to the point, lack of conclusive interpretable results, clearly demonstrate the complex and irreproducible catalytic activity of bis(imino) pyridine iron alkoxides with respect to lactide polymerization; such conflicting results clearly hinder the characterization and investigation of the catalytic activity of these iron (II) complexes, but despite extensive attempts we were not able to identify the sources of the problems observed.

Chapter 4

Summary and Conclusions

4.1 Synthesis of iron (II) complexes with N-benzyl substituents

The experimental work for the project presented in this manuscript commenced with the synthesis of iron (II) complexes based on bis(imino) pyridine ligands bearing *N*-alkyl substituents; as such, the first ligand that was considered for these synthetic procedures was 2,6-bis[(benzylimino)ethyl]pyridine. The literature data gave no indication regarding the formation of homoleptic bis(ligand) cationic species from a combination of iron (II) and this ligand. In fact, characterization data such as elemental analysis did nothing more than to corroborate the formation of the resulting heteroleptic iron (II) complexes, with the general formula (Ligand)FeX_2.

The mass spectrometry data pointed to the formation of the homoleptic ion-pair complexes. Crystallographic data, which was later obtained on these complexes and their tetraphenyl borate derivative, provided not only a firm corroboration to the formation of the homoleptic species, but also an insight as to the flexibility of the *N*-benzyl substituted bis(imino) pyridine ligand framework and its configuration around the metal center within the iron complex itself.

Within the general context of characterizing these homoleptic iron (II) complexes, nuclear magnetic resonance spectroscopy proved to be ineffective, since the formation of an homoleptic ion-pair complex also encompassed the formation of the paramagnetic tetrahedral

iron (II) dianionic species. Nevertheless, characterization of these complexes with UV-vis spectroscopy was both instructive and efficient; indeed, the low-energy transitions of these molecules proved to be highly similar, if not almost identical, both in terms of energy ranges, as well as molar absorbances.

Following these results, it became interesting to see if reaction with alkoxide or aryl oxide anions could convert the homoleptic ion-pair complexes to the desired heteroleptic, charge-neutral Fe-OR species. Attempts in this direction proved unsuccessful, however. The experimental work with *N*-benzyl substituted bis(imino) pyridine ligands not only revealed a paucity of literature data and characterization on the subject, but also indicated the elusive and subtle nature of iron chemistry, with respect to its coordination properties, as well as to its reactivity with alkyl and aryl oxide salts.

4.2 Synthesis of iron (II) complexes with N-aryl substituents

The above findings prompted us to reconsider our synthetic strategies to ensure access to the desired heteroleptic iron (II) complexes. Literature accounts presented in the first chapter of this thesis provide many examples of heteroleptic species resulting from treating iron dichloride with *N*-aryl substituted bis(imino) pyridine ligands, with *ortho*-substituents on the aromatic imine moiety. After comparison of various reaction yields and literature accounts, 2,6-bis[(2,4,6-trimethylanilimino)]pyridine iron (II) dichloride was chosen as a precursor molecule for any salt metathesis reaction that would possibly provide the desired iron dialkoxide species.

Despite the numerous experimental conditions that were attempted for such a salt metathesis reaction, no isolable product could be obtained. Indication that a new product was

being generated throughout all the trials was indeed apparent and unmistakable: all reaction attempts displayed the disappearance of the characteristic deep-indigo-blue color of the bis(imino) pyridine iron dichloride complex, and the appearance of a deep-green solution from which a green precipitate could be obtained. Partial and inconclusive evidence was obtained through mass spectrometry measurements on these green precipitates, which confirmed the formation of the desired five-coordinate iron dialkoxide species, albeit no analytically pure product could be obtained.

After numerous attempts at crystallization, a single crystal was generated that confirmed the formation of a diaryl oxide iron (II) complex with a bis(imino) pyridine ligand; the five-coordinate geometry of this species was confirmed through an X-ray diffraction analysis. However, the difficulty in the experimental work surrounding this synthesis, as well as the literature accounts of similar attempts and difficulties, clearly demonstrate the problematic nature in isolating pure samples of five-coordinate iron (II) alkoxide complexes bearing bis(imino) pyridine ligands.

Moreover, during the various salt metathesis tryout experiments, we used a number of alkaline salts were used with different functionalities and anionic species, such as thiocyanate, benzoate, phthalimide and N-hyrdoxyphthalimide salts. Indication that new products were being generated throughout all these reactions was apparent through the color changes in the reaction mixture, as well as through UV-vis spectroscopy measurements on all resulting product solutions. However, none of these reactions provided any isolable products that could be characterized further, and experimental work in this direction was soon put to a halt.

4.3 Lactide Polymerization

In view of the synthetic results, the experimental procedure of lactide polymerization reactions was adapted to make use of *in-situ* produced iron alkoxide species. Unfortunately, the polymerization results provided both inconclusive and irreproducible results with regards to time-dependant polymerization conversion values, as well as kinetic and mechanistic profiling experiments that were achieved via proton NMR spectroscopy, GPC and MALDI mass spectrometry analysis.

Details on the various results and problematic aspects of the iron alkoxide catalyzed polymerization reactions are provided in Chapter 2 of this manuscript. It becomes clear that iron (II) alkoxide catalyst systems studied during the course of this project are not only elusive with regards to their synthesis, but also present complex and irreproducible catalytic activities, which render enough activity to make it considerably interesting for study, but also, to a measure, provide irreproducible and conflicting results that cast a deep questioning as to the nature of their catalytic mechanism and efficiency.

4.4 Perspectives

Upon reflection on all the results that were obtained, the work that was achieved and the conclusions that were reached throughout this project, two possible courses and perspectives could be suggested within the framework of the study and catalytic utility of iron (II) alkoxide complexes. Firstly, it is indeed quite obvious and apparent that, despite the plentiful literature accounts on the chemistry of bis(imino) pyridine iron dichloride complexes, our understanding of the chemistry itself of these metal compounds remains extremely limited when applied to

alkoxide or aryl oxide ligands. All the above mentioned evidence testifies that there are still a great number of questions that remain unanswered, and numerous experimental trials and tests that need to be performed on heteroleptic bis(imino) pyridine iron (II) complexes bearing different functionalities before we achieve a full understanding of these molecules and their reactivity. For instance, literature accounts presented in the first chapter of this manuscript testify that protonation routes might present slightly more reliable synthetic pathways for obtaining five-coordinate iron (II) bis(alkoxide) complexes, in comparison with salt metathesis reactions that were attempted in this project.

Secondly, in view of the unreliable polymerization results that were obtained with our five-coordinate iron (II) catalyst, it becomes interesting to investigate iron (II) systems that present a higher level of coordinative unsaturation around the metal center. Anionic ligands such as bis(imino) pyrrole or bis(imino) benzene for instance might offer an interesting framework that would not only allow the formation of a four-coordinate iron (II) complex, but also the possibility of having only one alkoxide ligand on the metal center, thereby ensuring a simpler and more reliable polymerization mechanism.

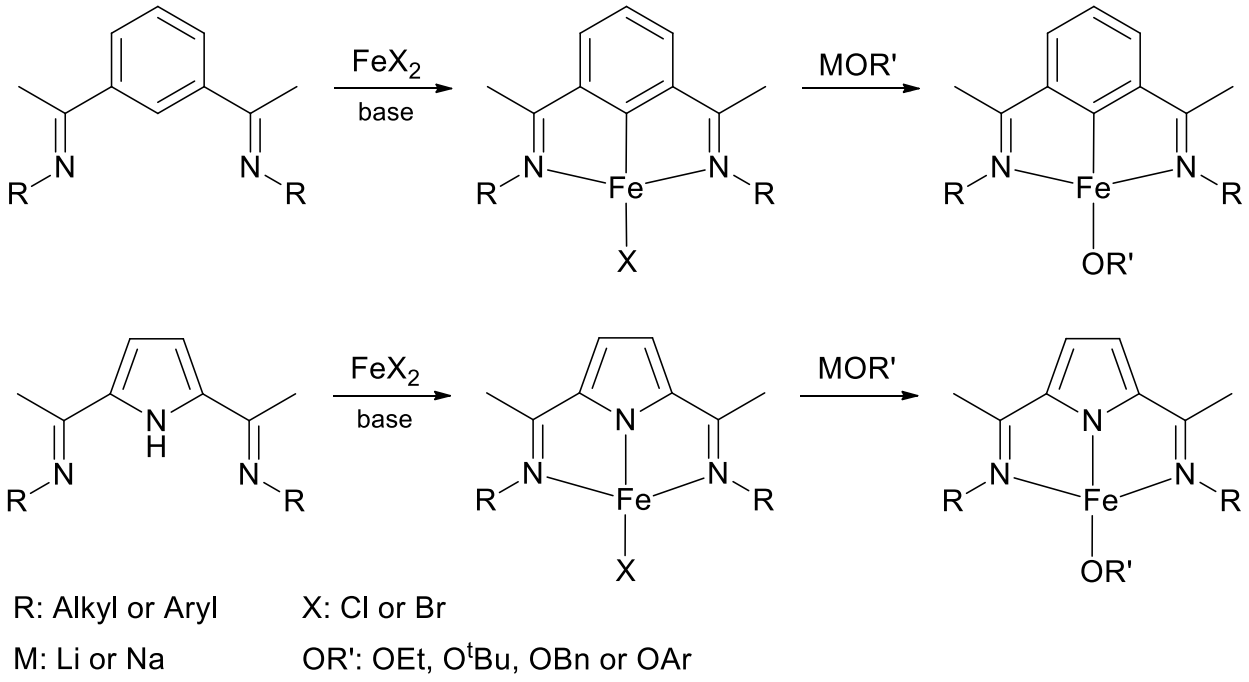

Scheme 4.1: Proposed schemes for the synthesis of iron (II) alkoxide catalysts.

It is only after such investigations and experimental endeavors are accomplished that we shall either be knowledgeable enough to efficiently apply iron (II) complexes within the framework of lactide polymerization, or else we shall be relieved from the opinion that we actually understand these molecules adequately.